Tampere University

Panu Keskinen

ANALYTICAL CALCULATION OF TOPOLOGICAL INVARIANTS FOR FOUR-BAND SYSTEMS

Faculty of Engineering and Natural Sciences
Master of Science Thesis
April 2021

ABSTRACT

Panu Keskinen: Analytical calculation of topological invariants for four-band systems
Master of Science Thesis
Tampere University
Science and Engineering
April 2021

In this thesis topological insulators are examined. Topology is a subfield of mathematics, which studies the properties of geometric objects under smooth deformations. We can define topological invariants for these objects, which remain constant under the deformations. Topological insulators are fundamentally different from conventional insulators. The bulk of the system acts as an insulator, but they have conducting surface states. The conductivity of the surface is quantized, which is related to the value of the topological invariant.

The main goal of this thesis is the analytical calculation of topological invariants for four-band systems. Performing the calculations analytically would give deeper insight into the properties of the system.

In the first part of the thesis, the theoretical background behind conventional insulators is recapped. The general Hamiltonian in the second quantization formalism is introduced. Then topological insulators and their topological invariants are examined.

The second part focuses on two-band Chern insulators. This type of system is described by a Hamiltonian, which is a Hermitian 2×2 matrix. It can be expressed as a linear combination of the identity matrix and the three Pauli matrices. The topological invariant corresponding to the Chern insulator is the Chern number, which can be analytically calculated. The invariant is integer-valued, where zero corresponds with the topologically trivial phase.

The next section focuses on four-band $\mathbb{Z}_2$ invariants. The Hamiltonian of such a system is a Hermitian 4×4 matrix. The basis is formed by the identity matrix, 5 Dirac gamma matrices and their 10 commutators. If the Hamiltonian can be turned into a block diagonal form, it reduces to two uncoupled Chern insulators. This allows the analytical calculation of the $\mathbb{Z}_2$ invariant, since it can be deduced by comparing the Chern numbers of these two systems. This invariant can only have a value of 0 or 1, which correspond to the trivial and topological phase.

The system can not generally be block diagonalized, but it is possible in certain special cases. These correspond to cases, where the Hamiltonian only has either time reversal symmetry or inversion symmetry breaking terms, which are mutually anticommuting.

The methods outlined before are applied to a few example systems. These include the Kane-Mele model, Bi_2Se_3, diamond and the BHZ model. For each system, the $\mathbb{Z}_2$ invariant is calculated and plotted as a function of some parameter of the Hamiltonian such that topological and trivial phases emerge.

Keywords: topological insulator, Chern insulator, Chern number, Z2 insulator, Z2 invariant

TIIVISTELMÄ

Panu Keskinen:
Diplomityö
Tampereen yliopisto
Teknis-luonnontieteellinen
Huhtikuu 2021

Tässä työssä tarkastellaan topologisia eristeitä. Topologia on matematiikan osa-alue, joka tutkii sileiden muutosten vaikutusta geometristen kappaleiden ominaisuuksiin. Kappaleille voidaan määrittää topologisia invariantteja, jotka pysyvät vakiona muutosten alla. Topologiset eristeet eroavat perustavanlaatuisesti tavallisista eristeistä. Tällaisten systeemien bulkki on kuten eriste, mutta niihin muodostuu johtavia pintatiloja. Pinnan johtavuus on kvantittunut, joka liittyy topologisen invariantin arvoon.

Työn päätavoitteena on laskea analyyttisesti topologisia invariantteja neljän energiavyön systeemeille. Analyyttinen laskeminen antaisi syvempää tietämystä systeemin ominaisuuksista.

Työn ensimmäisessä osassa käydään läpi yleistä teoriaa tavallisista eristeistä. Yleinen Hamiltonin operaattori esitellään toisen kvantisaation formalismissa. Tämän jälkeen käsitellään topologiset eristeet ja niiden topologiset invariantit.

Toisessa osassa keskitytään kahden energiavyön Chern-eristeisiin. Tällaista systeemiä kuvaa Hamiltonin operaattori, joka on hermiittinen 2×2 matriisi. Se voidaan esittää identiteettimatriisin sekä 3:n Paulin matriisin lineaarikombinaationa. Chern-eristettä vastaava topologinen invariantti on nimeltään Chernin luku, ja se voidaan laskea analyyttisesti. Invariantti voi olla arvoltaan mikä tahansa kokonaisluku, missä nolla vastaa topologisesti triviaalia faasia.

Seuraavassa osassa keskitytään neljän energiavyön $\mathbb{Z}_2$-eristeisiin. Tämän systeemin Hamilton on hermiittinen 4×4 matriisi. Tällaisille matriiseille muodostaa kannan identiteettimatriisi, 5 gammamatriisia sekä niiden 10 kommutaattoria. Jos Hamiltonin matriisi saadaan blokkidiagonaaliseen muotoon, niin se redusoituu kahdeksi kytkeytymättömäksi Chernin eristeeksi. Tämä mahdollistaa myös $\mathbb{Z}_2$-invariantin analyyttisen laskemisen, sillä se saadaan vertailemalla näiden kahden systeemin Chernin lukuja keskenään. Tämä invariantti voi saada vain arvot 0 ja 1, jotka vastaavat triviaalia ja topologista faasia.

Systeemiä ei yleisesti voi saada blokkidiagonaaliseen muotoon, mutta tietyissä erityistapauksissa se on mahdollista. Nämä vastaavat tapauksia, missä Hamiltonissa on joko vain ajankääntösymmetrian tai inversiosymmetrian rikkovia termejä, jotka ovat keskenään antikommutoivia.

Esiteltyjä menetelmiä sovelletaan muutamaan esimerkkisysteemiin. Näihin lukeutui Kane-Mele -malli, Bi_2Se_3, timantti sekä BHZ-malli. Jokaiselle systeemille lasketaan $\mathbb{Z}_2$-invariantti, joka piirretään jonkin parametrin funktiona siten että ilmenee sekä topologinen että triviaali faasi.

Avainsanat: topologinen eriste, Chern-eriste, Chernin luku, Z2-eriste, Z2-invariantti

CONTENTS

LIST OF FIGURES

LIST OF TABLES

1 INTRODUCTION

Topology is a branch of mathematics which studies the properties of geometric objects under smooth deformations. This means the deformation is done continuously without cutting or gluing. Properties which stay the same under these deformations are called topological invariants. For example, the number of holes in an object is a topological invariant which can only have non-negative integer values. Objects with the same value for the topological invariant belong to the same equivalence class. A common joke goes that a topologist can not tell the difference between a coffee cup and a donut, as they have the same number of holes! This fact is demonstrated in Figure 1.1.

The study of topological insulators combines condensed matter physics with topology. The properties of these materials are defined by some integer-valued topological invariant. With topological insulators, a smooth deformation corresponds to perturbing the band structure such that the band gap does not close. The band gap of an insulator is the energy range separating the valence band and the conductance band. When the gap closes, the system may undergo a quantum phase transition. If the state corresponds to a classical insulator for some value of the topological invariant, it is said to be in a trivial phase. Otherwise the system is in a topological phase.

The study of topological insulators began with the experimental discovery of the integer quantum Hall (IQHE) effect in 1980 by Klaus von Klitzing [1]. It was shown that the Hall conductance of a two-dimensional system subjected to a strong magnetic field can only

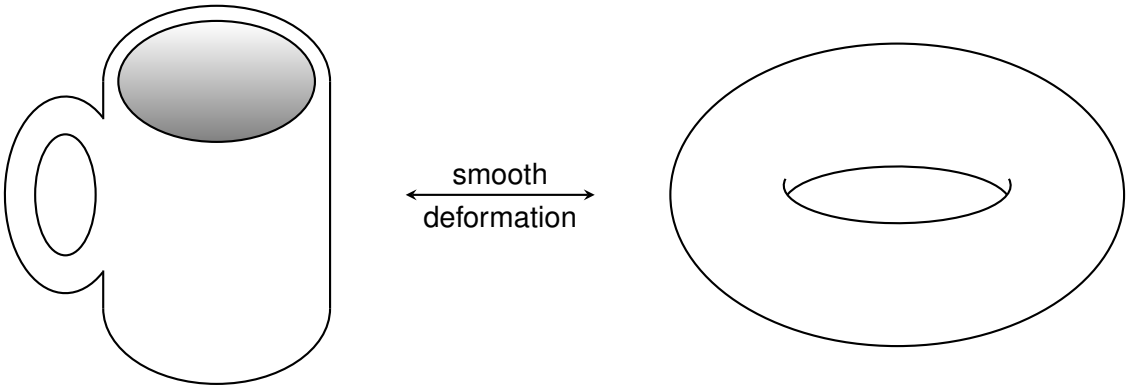

Figure 1.1. *The cup and the donut are topologically equivalent since one can be smoothly deformed into the other. The number of holes remains constant, as it is a topological invariant.*

have discrete values. Increasing the magnetic field, the Hall conductance plateaus and jumps up at certain intervals, resembling a staircase. The exact values for the plateaus are

$$\sigma_{xy} = c\frac{\mathrm{e}^2}{\mathrm{h}}, \quad c = 1, 2, 3, \ldots \tag{1.1}$$

where e is the elementary charge and h the Planck constant. The factor c is a topological invariant called the Chern number. The value corresponds to the number of conducting electrons on the edge of the sample. This means that the bulk acts as an insulator but the surface as a conductor. The 1985 Nobel Prize in Physics was awarded to von Klitzing for this discovery [2].

Because the Chern number is known to an integer from the topological reasoning, the Von Klitzing constant h/e^2 can be measured extremely precisely. In fact, it is now used to define the SI unit of resistance, the ohm. Using this value and another precisely measured quantity, the Josephson constant, the Planck constant can be determined. As a consequence, it is also used to define the SI unit of mass, the kilogram. [3]

The Chern number is only defined for two-dimensional systems. Furthermore, it requires that the time reversal (TR) symmetry is broken, for example by an external magnetic field such as in the case of the original IQHE experiment. For systems with unbroken TR symmetry, another topological invariant can be defined, called the $\mathbb{Z}_2$ invariant. It may only have two values, 0 or 1, corresponding to a trivial and a topological phase. The topological phase has two electrons on the edge, circling in opposite directions. Luckily, the $\mathbb{Z}_2$ invariant also generalizes to higher dimensions. This allows the existence of three-dimensional topological insulators.

As of now, most topological insulators require extremely cold temperatures, close to absolute zero. Alternatively, they require a strong magnetic field, such as in the case of the quantum Hall effect. Work has been done to achieve topological properties in higher temperatures. The goal is to achieve it in room temperature so that it may be used in ordinary household electronics. Some materials have been discovered, which have suitable properties for room temperature applications, such as Bi_2Se_3. [4] However, there is a long way to go before any practical applications of these ideas.

Topological insulators have lots of attractive properties for electronics. Due to the surface states being topologically protected, backscattering is prevented leading to dissipationless charge transport. In practice, this means there is no energy lost to heat from the electric current. [5] This could lead to devices with extremely high energy efficiencies, allowing higher performance with lower power consumption. Some fields of study where the applications of topological materials seem especially promising include thermoelectornics [6], nanoelectronics and optoelectronics [7].

Topological materials may also prove to be useful in quantum computing. Current realizations of quantum computers are extremely sensitive to external influences, causing the decoherence of the quantum state. This makes them useless for any practical tasks since only a small amount of qubits can be held in a coherent state. Even then, the tem-

perature must be kept close to absolute zero to minimize to effect of thermal energy. In addition, a true quantum computer would require error correction, massively increasing the number of qubits needed. Since topological states are by definition stable under local perturbations, they could potentially be used as qubits. [8] This would allow for larger quantum computers to be built.

The Chern number of a two-band system can be easily calculated analytically. This aim of this thesis is to derive analytical formulas for calculating the $\mathbb{Z}_2$ invariant for four-band systems. This is possible when the Hamiltonian of the system can be block diagonalized. In this case, the system reduces to two uncoupled Chern insulators. Then a nonzero $\mathbb{Z}_2$ invariant corresponds to different Chern numbers between these two systems. This is not possible to do in the general case. Any 4×4 Hermitian matrix can be expressed as a linear combination of the identity matrix, 5 Dirac gamma matrices and their 10 commutators. These matrices also form the three-dimensional analogue of the Pauli matrices. If all of these terms have nonzero coefficients, then the block diagonalization is not possible. In certain circumstances, it is possible when up to 7 of these terms are present. The performing a unitary transformation and choosing a suitable representation for the gamma matrices can transform the Hamiltonian into a block diagonal form.

The theoretical background behind the topic of this thesis is explained in Chapter 2. The first section focuses on ordinary insulators. The second part introduces the concept of topological insulators. Some example systems are demonstrated for both. Chapter 3 focuses on two-band Chern insulators and the mathematical structure of the models. Analytical formulas are divided for calculating the Chern number for such systems. Chapter 4 moves on to four-band $\mathbb{Z}_2$ insulators. The general procedure behind the block diagonalization of the Hamiltonian is shown. The cases with TR breaking and I breaking terms in the Hamiltonian are analyzed. In Chapter 5, numerical results are shown for certain models of topological insulators.

2 THEORETICAL BACKGROUND

2.1 Theory of solids

2.1.1 Band structure

The electrical properties of a solid are determined by its band structure. The band structure shows the allowed energy levels for the electrons in the solid. The energy levels form densely occupied energy bands but also gaps where the corresponding energies are not allowed. For an electron to cross from one band to another, it needs enough energy to cross this gap. In the ground state, the electrons are in the lowest possible energy configuration so the bands are filled from the bottom up to the Fermi level E_F.

Traditionally solids can be divided into four categories based on their band structure:

- insulators
- semiconductors
- semimetals
- metals.

For insulators, the Fermi level lies between the valence band and the conduction band. They are separated by the band gap, which determines the energy required to excite an electron from the valence band to the conduction band. The general form of the band structure is shown in Figure 2.1. If the band gap is small, the material is a semiconductor. This means that thermal energy is enough to excite electrons from the valence band to the conduction band. The conductivity thus depends on the temperature of the system. In metals there is no band gap at the Fermi level so they are good conductors of electricity. In such systems the conducting electrons can be modelled as an electron gas. In semimetals there is only a small overlap between the valence and conduction bands. These materials conduct electricity but do it rather poorly.

Another way to classify insulators and conductors is by observing the locality of the ground state wave function. In an insulator, the wave function is localized. This means that the electron is with high probability contained near the atomic nucleus and outside of this region the wave function decays exponentially. Long range effects are thus not possible and the system is not sensitive to boundary conditions. In a conductor, the opposite

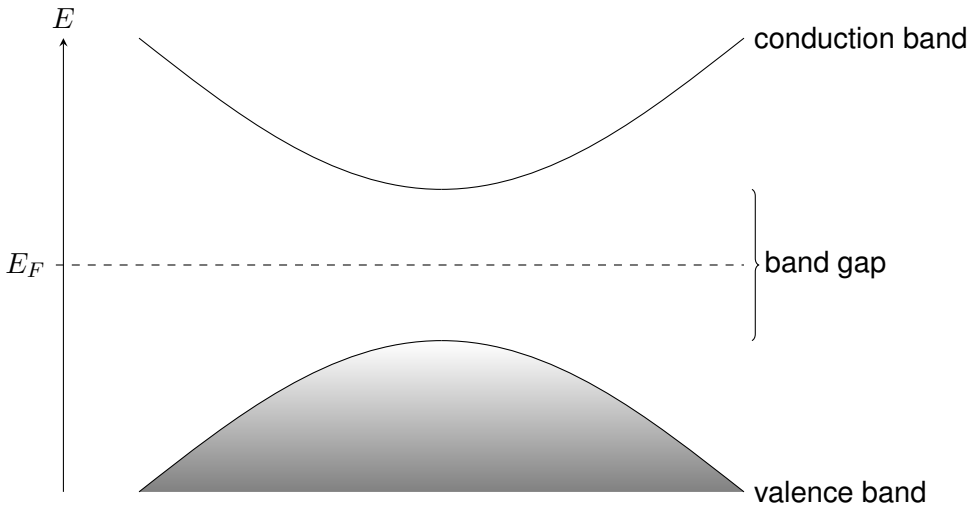

Figure 2.1. *The general band structure of an insulator. The energy levels are filled up to the Fermi level E_F.*

is true: the wave function is delocalized. This allows charge carriers to move freely within the system.

Every ordinary insulator is similar in the sense that the band structure of one can be smoothly deformed into that of an other without closing the band gap at any point in the process. This means they belong to the same topological equivalence class. The only notable difference is the size of the band gap, which describes how well insulating the material is. In this sense, they are also equivalent to the vacuum, which has the maximum band gap. There is also another class of insulators which are not topologically equivalent to the vacuum. These are called topological insulators.

2.1.2 Second quantization

In the first quantization formalism, the state of a single particle is represented by a complex wavefunction varied in space. The state of a system with N particles may thus be represented by listing the state of each individual particle. This representation does, however, have some redundant information. Because of the indistinguishability principle, it is in fact not possible to know the state of each individual particle. A more accurate description is to talk about the number of occupants per each state. This is called second quantization or the occupation number representation. [9]

Using second quantization formalism, a many-particle system can be written quite succinctly. Using Dirac's notation, the occupation number of each state can be listed inside a ket. The state of an N-particle system is thus

$$|n_1, n_2, n_3, \ldots\rangle, \quad \sum_i n_i = N, \tag{2.1}$$

where n_i is the occupation number of state i. For bosons this may be any non-negative

integer, but for fermions it is limited to 0 or 1. Going forward, we will focus on fermionic systems. The fundamental operators used in second quantization are the creation and annihilation operators. The fermionic creation operator $c_i^\dagger$ increases the occupation number of state i by one, whereas the annihilation operator c lowers it by one:

$$\begin{aligned} c_i^\dagger \left|\ldots, n_{i-1}, n_i, n_{i+1}, \ldots\right\rangle &= \left|\ldots, n_{i-1}, n_i + 1, n_{i+1}, \ldots\right\rangle, \\ c_i \left|\ldots, n_{i-1}, n_i, n_{i+1}, \ldots\right\rangle &= \left|\ldots, n_{i-1}, n_i - 1, n_{i+1}, \ldots\right\rangle. \end{aligned} \tag{2.2}$$

Acting on an already occupied state with the creation operator annihilates the state completely. Likewise for acting on an unoccupied state with the annihilation operator:

$$c_i^\dagger \left|\ldots, n_{i-1}, 1, n_{i+1}, \ldots\right\rangle = 0, \quad c_i \left|\ldots, n_{i-1}, 0, n_{i+1}, \ldots\right\rangle = 0. \tag{2.3}$$

Because of this property, the operators are clearly not commutative. They satisfy the commutation relations

$$\{c_i^\dagger, c_j^\dagger\} = 0, \quad \{c_i, c_j\} = 0, \quad \{c_i, c_j^\dagger\} = \delta_{ij}, \tag{2.4}$$

where δ_{ij} is the Kronecker delta. All other second quantization operators may be expressed by using the creation and annihilation operators. For example, the occupation number operator can be written as

$$\hat{n}_i = c_i^\dagger c_i \tag{2.5}$$

for state i. A general one-particle operator is given by

$$T_{\text{tot}} = \sum_{ij} T_{ij} c_i^\dagger c_j, \tag{2.6}$$

where T_{ij} describers the strength of the coupling between states i and j. Examples of one-particle operators are the kinetic energy operator or an external potential. Similarly, a general two-particle operator is given by

$$V_{\text{tot}} = \frac{1}{2} \sum_{ijkl} V_{ijkl} c_i^\dagger c_j^\dagger c_l c_k, \tag{2.7}$$

where V_{ijkl} is the strength of the interaction. This may be, for example, the Coulomb potential. The factor of one half is to account for double counting.

2.1.3 Reciprocal lattice

The atoms of a solid are on a periodic lattice called a Bravais lattice. This means the system has translational invariance. Any point in the lattice is given by the linear combination

$$\boldsymbol{R} = n_1 \boldsymbol{a}_1 + n_2 \boldsymbol{a}_2 + n_3 \boldsymbol{a}_3, \quad n_1, n_2, n_3 \in \mathbb{Z}, \tag{2.8}$$

where $\boldsymbol{a}_1, \boldsymbol{a}_2, \boldsymbol{a}_3$ are the lattice vectors. The parallelepiped formed by the lattice vectors is a primitive unit cell of the system. Another choice for the unit cell is the Wigner-Seitz cell. It is obtained by taking all points closer to the central atom than any other atom.

According to Bloch's theorem, the wavefunction of an electron in a periodic potential can be written as the product of a plane wave and a lattice periodic function

$$\psi(\boldsymbol{r}) = u(\boldsymbol{r})\mathrm{e}^{\mathrm{i}\boldsymbol{k}\cdot\boldsymbol{r}}, \quad u(\boldsymbol{r}+\boldsymbol{R}) = u(\boldsymbol{r}), \tag{2.9}$$

where $\boldsymbol{k}$ is the crystal momentum. Now it is possible to take a Fourier transformation from the position space to the reciprocal space, also known as $\boldsymbol{k}$-space. This defines a new lattice called the reciprocal lattice, which is periodic with respect to the $\boldsymbol{k}$-vector. The points of this lattice are given by

$$\boldsymbol{G} = m_1\boldsymbol{b}_1 + m_2\boldsymbol{b}_2 + m_3\boldsymbol{b}_3, \quad m_1, m_2, m_3 \in \mathbb{Z}, \tag{2.10}$$

where $\boldsymbol{b}_1, \boldsymbol{b}_2, \boldsymbol{b}_3$ are the reciprocal lattice vectors satisfying

$$\boldsymbol{a}_i \cdot \boldsymbol{b}_j = 2\pi\delta_{ij}. \tag{2.11}$$

The Wigner-Seitz cell of the reciprocal lattice is called the Brillouin zone (BZ). The BZ closest to the origin is defined as the First Brillouin Zone (FBZ). For any value of $\boldsymbol{k}$ outside of the FBZ, there is a corresponding value inside it, such that they differ by some $\boldsymbol{G}$ as given in equation 2.10. This means that the properties of the whole system are contained in the FBZ. From now on the FBZ is simply referred to as the BZ.

2.1.4 Tight binding model

The Hamiltonian for non-interacting electrons on a Bravais lattice in the second quantization formalism is

$$H = \sum_{i,\sigma} \epsilon_i c_{i\sigma}^\dagger c_{i\sigma} - \sum_{i,j,\sigma} t_{ij} c_{i\sigma}^\dagger c_{j\sigma}, \tag{2.12}$$

where ϵ_i is the on-site energy for site i and t_{ij} the hopping integral between sites i and j. Each site additionally has two states corresponding to the electron spin: $\sigma = \uparrow, \downarrow$ for spin-up and spin-down. The creation and annihilation operators for an electron with spin σ at site i are denoted by $c_{i\sigma}^\dagger$ and $c_{i\sigma}$, respectively. Any spin-orbit coupling is neglected in this model.

The tight binding model assumes that the electrons are highly localized to the atomic nuclei. This means that usually only the interactions between nearest-neighbor (or sometimes next-nearest-neighbor) sites are considered. Let us assume that the hopping integral is identical between any neighboring sites, such that $t_{ij} = t$. For any other two sites, the hopping is assumed to be zero. The on-site energy is also assumed to be identical

for each site such that $\epsilon_i = \epsilon$. Now the tight-binding Hamiltonian can be written as

$$H = \epsilon \sum_{j,\sigma} c_{j\sigma}^\dagger c_{j\sigma} - t \sum_{\langle ij \rangle,\sigma} c_{i\sigma}^\dagger c_{j\sigma}. \tag{2.13}$$

The operator $c_{j+\boldsymbol{\delta}}$ corresponds to the creation operator for the site displaced from site j by the vector $\boldsymbol{\delta}$. This Hamiltonian is given in the position basis. To change over to the reciprocal space, we need to perform the Fourier transform

$$c_{j\sigma} = \frac{1}{\sqrt{N}} \sum_{\boldsymbol{k}} \mathrm{e}^{\mathrm{i}\boldsymbol{k}\cdot\boldsymbol{R}_j} c_{\boldsymbol{k}\sigma}, \tag{2.14}$$

where N is the total number of sites in the lattice and $\boldsymbol{R}_j$ the position of site j. The creation operator for the site corresponding to the crystal momentum $\boldsymbol{k}$ and spin σ is denoted by $c_{\boldsymbol{k}\sigma}$. Plugging this into the first term gives simply

$$\epsilon \sum_{\boldsymbol{k},\sigma} c_{\boldsymbol{k}\sigma}^\dagger c_{\boldsymbol{k}\sigma} \tag{2.15}$$

The second term can be written as

$$-t \sum_{j,\sigma} \sum_{\boldsymbol{\delta}} c_{j+\boldsymbol{\delta},\sigma}^\dagger c_{j\sigma} + c_{j\sigma}^\dagger c_{j+\boldsymbol{\delta},\sigma}, \tag{2.16}$$

where $\boldsymbol{\delta}$ ranges over the nearest-neighbor vectors. Performing the Fourier transform turns this into

$$\begin{aligned}
H &= -\frac{t}{N} \sum_{j,\sigma} \sum_{\boldsymbol{\delta}} \sum_{\boldsymbol{k},\boldsymbol{k}'} \mathrm{e}^{-\mathrm{i}\boldsymbol{k}\cdot(\boldsymbol{R}_j+\boldsymbol{\delta})} \mathrm{e}^{\mathrm{i}\boldsymbol{k}'\cdot\boldsymbol{R}_j} c_{\boldsymbol{k}\sigma}^\dagger c_{\boldsymbol{k}'\sigma} + \mathrm{e}^{-\mathrm{i}\boldsymbol{k}\cdot\boldsymbol{R}_j} \mathrm{e}^{\mathrm{i}\boldsymbol{k}'\cdot(\boldsymbol{R}_j+\boldsymbol{\delta})} {c_{\boldsymbol{k}\sigma}}^\dagger c_{\boldsymbol{k}'\sigma} \\
&= -\frac{t}{N} \sum_{\sigma} \sum_{\boldsymbol{\delta}} \sum_{\boldsymbol{k},\boldsymbol{k}'} (\mathrm{e}^{-\mathrm{i}\boldsymbol{k}\cdot\boldsymbol{\delta}} + \mathrm{e}^{\mathrm{i}\boldsymbol{k}'\cdot\boldsymbol{\delta}}) \sum_{j} \mathrm{e}^{\mathrm{i}(\boldsymbol{k}'-\boldsymbol{k})\cdot\boldsymbol{R}_j} c_{\boldsymbol{k}\sigma}^\dagger c_{\boldsymbol{k}'\sigma} \\
&= -t \sum_{\sigma} \sum_{\boldsymbol{\delta}} \sum_{\boldsymbol{k},\boldsymbol{k}'} (\mathrm{e}^{-\mathrm{i}\boldsymbol{k}\cdot\boldsymbol{\delta}} + \mathrm{e}^{\mathrm{i}\boldsymbol{k}'\cdot\boldsymbol{\delta}}) \delta_{\boldsymbol{k}\boldsymbol{k}'} c_{\boldsymbol{k}\sigma}^\dagger c_{\boldsymbol{k}'\sigma} \\
&= -t \sum_{\sigma} \sum_{\boldsymbol{\delta}} \sum_{\boldsymbol{k}} (\mathrm{e}^{\mathrm{i}\boldsymbol{k}\cdot\boldsymbol{\delta}} + \mathrm{e}^{-\mathrm{i}\boldsymbol{k}\cdot\boldsymbol{\delta}}) c_{\boldsymbol{k}\sigma}^\dagger c_{\boldsymbol{k}\sigma} \\
&= -t \sum_{\boldsymbol{k},\sigma} \sum_{\boldsymbol{\delta}} \cos(\boldsymbol{k}\cdot\boldsymbol{\delta}) c_{\boldsymbol{k}\sigma}^\dagger c_{\boldsymbol{k}\sigma},
\end{aligned} \tag{2.17}$$

where the handy relation

$$\frac{1}{N} \sum_{j} \mathrm{e}^{\mathrm{i}(\boldsymbol{k}'-\boldsymbol{k})\cdot\boldsymbol{R}_j} = \delta_{\boldsymbol{k}\boldsymbol{k}'} \tag{2.18}$$

has been used. Now that the Hamiltonian has been diagonalized, the energy dispersion is easily seen to be

$$E(\boldsymbol{k}) = -t \sum_{\boldsymbol{\delta}} \cos(\boldsymbol{k}\cdot\boldsymbol{\delta}). \tag{2.19}$$

This is a typical way to examine a system in the second quantization formalism.

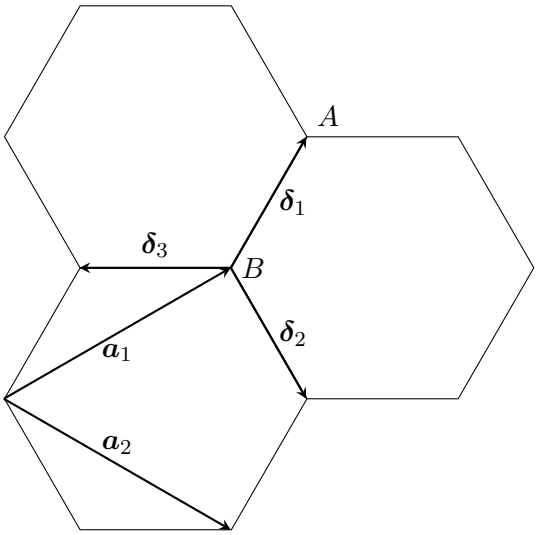

Figure 2.2. *The hexagonal graphene lattice with lattice vectors $\boldsymbol{a}_1$, $\boldsymbol{a}_2$ and nearest-neighbor vectors $\boldsymbol{\delta}_1$, $\boldsymbol{\delta}_2$, $\boldsymbol{\delta}_3$. The unit cell consists of two sites: A and B.*

2.1.5 Graphene

The first models for topological insulators were based on graphene. For this reason, it is of interest to first study a simpler non-topological model of it. Graphene consists of a 2-dimensional sheet of carbon atoms in a honeycomb lattice. This is a hexagonal bipartite lattice so each unit cell comprises of two atoms. The different sites in the unit cell are denoted by A and B. The lattice vectors are

$$\boldsymbol{a}_1 = \frac{a}{2}\begin{pmatrix} 3 \\ \sqrt{3} \end{pmatrix}, \quad \boldsymbol{a}_2 = \frac{a}{2}\begin{pmatrix} 3 \\ -\sqrt{3} \end{pmatrix}, \tag{2.20}$$

where a is the lattice constant corresponding to the distance between A and B sites. The electron spin is ignored for now, which corresponds to a particle-hole symmetry for the system. This is not physical but is done for convenience. The spin will be restored later on in more complicated models for topological insulators. The simplest Hamiltonian for this system only has one term corresponding to the hopping between nearest-neighbor sites

$$H = -t \sum_{j,\boldsymbol{\delta}} c^\dagger_{Aj} c_{B,j+\boldsymbol{\delta}} + c^\dagger_{B,j+\boldsymbol{\delta}} c_{Aj}, \tag{2.21}$$

where the hopping parameter t is assumed to be equal between any two neighboring sites. The operators $c^{(\dagger)}_{A\boldsymbol{k}}$ and $c^{(\dagger)}_{B\boldsymbol{k}}$ are the annihilation (creation) operators for sites A and B corresponding to the crystal momentum $\boldsymbol{k}$. The nearest-neighbor vectors from site B to the A sites are given in terms of the lattice vectors as

$$\boldsymbol{\delta}_1 = \frac{2\boldsymbol{a}_1 - \boldsymbol{a}_2}{3}, \quad \boldsymbol{\delta}_2 = \frac{2\boldsymbol{a}_2 - \boldsymbol{a}_1}{3}, \quad \boldsymbol{\delta}_3 = -\frac{\boldsymbol{a}_1 + \boldsymbol{a}_2}{3}. \tag{2.22}$$

These are shown along with the lattice vectors in Figure 2.2. We shall perform a Fourier transform as given in equation 2.14. The Fourier transformed Hamiltonian is

$$\begin{aligned} H &= -\frac{t}{N}\sum_{j,\boldsymbol{\delta}}\sum_{\boldsymbol{k},\boldsymbol{k}'} \mathrm{e}^{-\mathrm{i}\boldsymbol{k}\cdot\boldsymbol{R}_j} c^\dagger_{A\boldsymbol{k}} \mathrm{e}^{\mathrm{i}\boldsymbol{k}'\cdot(\boldsymbol{R}_j+\boldsymbol{\delta})} c_{B\boldsymbol{k}'} + \mathrm{e}^{-\mathrm{i}\boldsymbol{k}\cdot(\boldsymbol{R}_j+\boldsymbol{\delta})} c^\dagger_{B\boldsymbol{k}} \mathrm{e}^{\mathrm{i}\boldsymbol{k}'\cdot\boldsymbol{R}_j} c_{A\boldsymbol{k}'} \\ &= -\frac{t}{N}\sum_{\boldsymbol{\delta}}\sum_{\boldsymbol{k},\boldsymbol{k}'} (\mathrm{e}^{\mathrm{i}\boldsymbol{k}'\cdot\boldsymbol{\delta}} c^\dagger_{A\boldsymbol{k}} c_{B\boldsymbol{k}'} + \mathrm{e}^{-\mathrm{i}\boldsymbol{k}\cdot\boldsymbol{\delta}} c^\dagger_{B\boldsymbol{k}} c_{A\boldsymbol{k}'}) \sum_j \mathrm{e}^{\mathrm{i}(\boldsymbol{k}'-\boldsymbol{k})\cdot\boldsymbol{R}_j} \\ &= -t\sum_{\boldsymbol{\delta}}\sum_{\boldsymbol{k},\boldsymbol{k}'} (\mathrm{e}^{\mathrm{i}\boldsymbol{k}'\cdot\boldsymbol{\delta}} c^\dagger_{A\boldsymbol{k}} c_{B\boldsymbol{k}'} + \mathrm{e}^{-\mathrm{i}\boldsymbol{k}\cdot\boldsymbol{\delta}} c^\dagger_{B\boldsymbol{k}} c_{A\boldsymbol{k}'}) \delta_{\boldsymbol{k}\boldsymbol{k}'} \\ &= -t\sum_{\boldsymbol{\delta},\boldsymbol{k}} c^\dagger_{A\boldsymbol{k}} \mathrm{e}^{\mathrm{i}\boldsymbol{k}\cdot\boldsymbol{\delta}} c_{B\boldsymbol{k}} + c^\dagger_{B\boldsymbol{k}} \mathrm{e}^{-\mathrm{i}\boldsymbol{k}\cdot\boldsymbol{\delta}} c_{A\boldsymbol{k}}. \end{aligned} \tag{2.23}$$

A useful way to write this Hamiltonian is in the so-called Bloch form

$$\sum_{\boldsymbol{k}} \boldsymbol{c}^\dagger_{\boldsymbol{k}} h(\boldsymbol{k}) \boldsymbol{c}_{\boldsymbol{k}}, \tag{2.24}$$

where $\boldsymbol{c}_{\boldsymbol{k}}$ is the basis formed by the annihilation operators for sites A and B and $h(\boldsymbol{k})$ is a 2×2 matrix periodic in the lattice such that $h(\boldsymbol{k}+\boldsymbol{b}_i) = h(\boldsymbol{k})$ for any reciprocal lattice vector $\boldsymbol{b}_i$. To get the graphene Hamiltonian in the Bloch form, we need to apply a phase change to one of the sites. This can be done via a unitary transformation so it does not affect the properties of the system. This is achieved by multiplying the site B annihilation operator by $\mathrm{e}^{\mathrm{i}\boldsymbol{k}\cdot\boldsymbol{\delta}_3}$. This results in the matrix

$$\begin{aligned} H &= \sum_{\boldsymbol{k}} \begin{pmatrix} c^\dagger_{A\boldsymbol{k}} & c^\dagger_{B\boldsymbol{k}} \end{pmatrix} \begin{pmatrix} 0 & -t\sum_{\boldsymbol{\delta}} \mathrm{e}^{\mathrm{i}\boldsymbol{k}\cdot\boldsymbol{\delta}} \\ -t\sum_{\boldsymbol{\delta}} \mathrm{e}^{-\mathrm{i}\boldsymbol{k}\cdot\boldsymbol{\delta}} & 0 \end{pmatrix} \begin{pmatrix} c_{A\boldsymbol{k}} \\ c_{B\boldsymbol{k}} \end{pmatrix} \\ &= \sum_{\boldsymbol{k}} \begin{pmatrix} c^\dagger_{A\boldsymbol{k}} & c^\dagger_{B\boldsymbol{k}} \end{pmatrix} \begin{pmatrix} 0 & -t(\mathrm{e}^{\mathrm{i}\boldsymbol{k}\cdot\boldsymbol{a}_1} + \mathrm{e}^{\mathrm{i}\boldsymbol{k}\cdot\boldsymbol{a}_2} + 1) \\ -t(\mathrm{e}^{-\mathrm{i}\boldsymbol{k}\cdot\boldsymbol{a}_1} + \mathrm{e}^{-\mathrm{i}\boldsymbol{k}\cdot\boldsymbol{a}_2} + 1) & 0 \end{pmatrix} \begin{pmatrix} c_{A\boldsymbol{k}} \\ c_{B\boldsymbol{k}} \end{pmatrix} \\ &= \sum_{\boldsymbol{k}} \boldsymbol{c}^\dagger_{\boldsymbol{k}} h(\boldsymbol{k}) \boldsymbol{c}_{\boldsymbol{k}}. \end{aligned} \tag{2.25}$$

Now the Hamiltonian can be written in the general form

$$h(\boldsymbol{k}) = d_0(\boldsymbol{k}) + \boldsymbol{d}(\boldsymbol{k})\cdot\boldsymbol{\sigma}, \tag{2.26}$$

where the coefficients are

$$\begin{aligned} d_0 &= 0 \\ d_1 &= -t(\cos(\boldsymbol{k}\cdot\boldsymbol{a}_1) + \cos(\boldsymbol{k}\cdot\boldsymbol{a}_2) + 1), \\ d_2 &= -t(\sin(\boldsymbol{k}\cdot\boldsymbol{a}_1) + \sin(\boldsymbol{k}\cdot\boldsymbol{a}_2)), \\ d_3 &= 0. \end{aligned} \tag{2.27}$$

and $\boldsymbol{\sigma}$ is the vector of Pauli matrices

$$\sigma_x = \begin{pmatrix} 0 & 1 \\ 1 & 0 \end{pmatrix}, \quad \sigma_y = \begin{pmatrix} 0 & -i \\ i & 0 \end{pmatrix}, \quad \sigma_z = \begin{pmatrix} 1 & 0 \\ 0 & -1 \end{pmatrix}. \tag{2.28}$$

This has the form of the two-dimensional Dirac equation for a massless particle. This is an extremely succinct and powerful way to describe any two-band system. The system is gapped for any value of $\boldsymbol{k}$ except for the high symmetry points in the corners of the Brillouin zone. These are labeled as

$$\boldsymbol{K} = \frac{2\pi}{3a}\begin{pmatrix} 1 \\ 1/\sqrt{3} \end{pmatrix}, \quad \boldsymbol{K'} = \frac{2\pi}{3a}\begin{pmatrix} 1 \\ -1/\sqrt{3} \end{pmatrix}. \tag{2.29}$$

We are interested in the energy dispersion around these points. Let us investigate the Hamiltonian around the point $\boldsymbol{K}$. By defining the function

$$\begin{aligned} f(\boldsymbol{k}) &= \mathrm{e}^{\mathrm{i}\boldsymbol{k}\cdot\boldsymbol{a}_1} + \mathrm{e}^{\mathrm{i}\boldsymbol{k}\cdot\boldsymbol{a}_2} + 1 \\ &= 2\mathrm{e}^{\mathrm{i}3a/2k_x}\cos\left(\frac{\sqrt{3}a}{2}k_y\right) \end{aligned} \tag{2.30}$$

we can take the first order approximation around $\boldsymbol{K}$

$$\begin{aligned} f(\boldsymbol{K}+\delta\boldsymbol{k}) &\approx f(\boldsymbol{K}) + \delta\boldsymbol{k}\cdot\nabla f(\boldsymbol{k})\Big|_{\boldsymbol{k}=\boldsymbol{K}} \\ &= \frac{3a}{2}(\delta k_y - \mathrm{i}\delta k_x) \end{aligned} \tag{2.31}$$

assuming that $\boldsymbol{k} \ll \boldsymbol{K}$. Setting $\frac{3at}{2} = 1$ and taking out the phase factor of $-\mathrm{i}$ gives the Hamiltonian

$$\begin{aligned} h(\boldsymbol{K}+\delta\boldsymbol{k}) &\approx \begin{pmatrix} 0 & \delta k_x - \mathrm{i}\delta k_y \\ \delta k_x + \mathrm{i}\delta k_y & 0 \end{pmatrix} \\ &= \delta k_x\sigma_x + \delta k_y\sigma_y, \end{aligned} \tag{2.32}$$

which has the form of a gapless Dirac Hamiltonian. Doing a similar expansion around the $\boldsymbol{K'}$ point yields

$$h(\boldsymbol{K'}+\delta\boldsymbol{k}) \approx -\delta k_x\sigma_x + \delta k_y\sigma_y \tag{2.33}$$

The touching of the bands suggests a conducting material. Since this only happens at points $\boldsymbol{K}$ and $\boldsymbol{K'}$, this classifies graphene as a semimetal. The conducting surface states are protected by both the TR and the I symmetry. However, the gap that opens up is only of the order of 10^{-6} eV. This is too small to be observed in realistic temperatures [10].

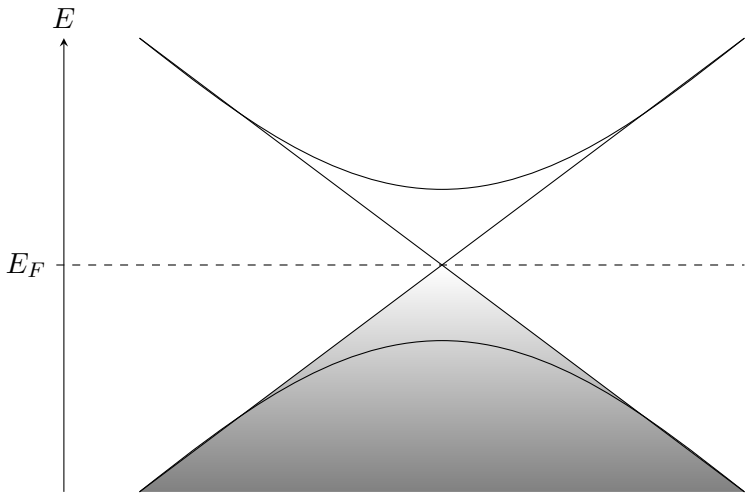

Figure 2.3. *Topological insulator with conducting surface states forming a Dirac cone.*

2.2 Topological insulators

The state of a topological insulator is divided into topologically trivial and nontrivial phases. The phase of the system is given by some topological invariant, which is usually integer-valued. The topological invariant is a type of quantum number, but it can be measured even in macroscopic systems. By varying some parameter of the Hamiltonian, the system can be driven to undergo a quantum phase transition, where the value of the topological invariant changes.

The bulk band structure of a topological insulator resembles that of a classical insulator, so it has a finite band gap. This band gap closes at some points in $\boldsymbol{k}$-space when the system undergoes a quantum phase transition. In the topological phase, there are conducting surface states, which are topologically protected. This means that the gap can not be closed by any small perturbation unless it breaks some underlying symmetry of the Hamiltonian. The symmetry which protects the surface states may be the TR of the I symmetry.

In a Chern insulator discrete symmetries of the system (typically TR or I) are broken by some internal properties of the system or by an external magnetic field, for example. The topological invariant describing the state of the system is the first Chern number. It corresponds to the number of conducting edge electrons. The Chern number is only defined for two-dimensional systems with broken TR symmetry. The Chern number is only defined for isolated bands, which are not touching any other bands. This means that during a quantum phase transition as the band gap is closed, the Chern number is not defined. Rather, there is a discontinuous jump from one value to an another.

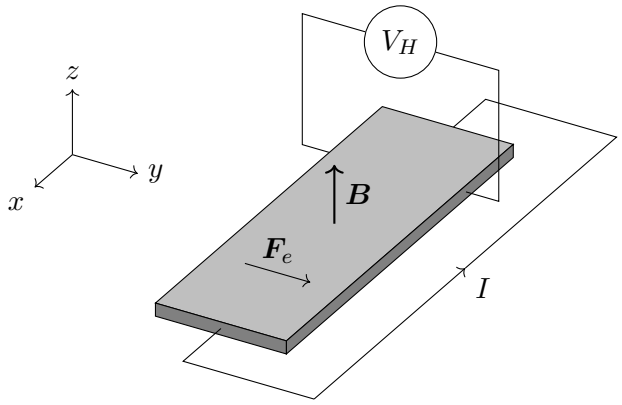

Figure 2.4. *The experimental setup for measuring the quantum Hall effect. Current I is driven through a thin sheet of material with magnetic field $\boldsymbol{B}$ applied perpendicular to the sample. The magnetic field causes the force $\boldsymbol{F}_e$ on the electrons.*

2.2.1 Quantum Hall effect

The ordinary Hall effect was discovered by Edwin H. Hall in 1879. He studied a two-dimensional sample with current I going through it in the x-direction, as shown in Figure 2.4. Then he applied a magnetic field $\boldsymbol{B}$ perpendicular to the sample, in the z-direction. The magnetic field causes the electrons to initially take a curved path via the Lorentz force $\boldsymbol{F}_e$. The charges build up on the edge of the sample causing a potential difference to form in the y-direction, which is called the Hall voltage V_H. The corresponding conductance is called the Hall conductance σ_{xy}, meaning the conductance in the y-direction as the current goes in the x-direction. Eventually the system reaches equilibrium as the charge build-up cancels the Lorentz force. After this point, the electrons take linear paths through the sample.

The integer quantum Hall effect (IQHE) was discovered by Klaus von Klitzing in 1980. He measured the Hall conductance of a semiconductor sample under a strong magnetic field. Surprisingly, the value did not smoothly increase with the magnetic field strength. Rather it seemed to plateau on certain values with rapid jumps inbetween. The plateaus were measured to be integer multiples of e^2 / h, showing that the Hall conductance was quantized. Even more surprisingly, the impurity of the sample did not diminish the effect but rather strengthened it. This meant that this quantum mechanical effect could be easily seen even in macroscopic samples. Figure 2.5 shows the Hall resistivity ρ_{xy} and the the longitudal resistivity ρ_{xx} as measured experimentally. The Hall resistivity can be seen to form plateaus at

$$\rho_{xy} = \frac{\mathrm{h}}{c\mathrm{e}^2}, \quad c = 1, 2, 3, \ldots \tag{2.34}$$

exhibiting the integer quantum Hall effect. This discovery earned von Klitzing the 1985 Nobel Prize in Physics and kicked off the study of topological insulators.

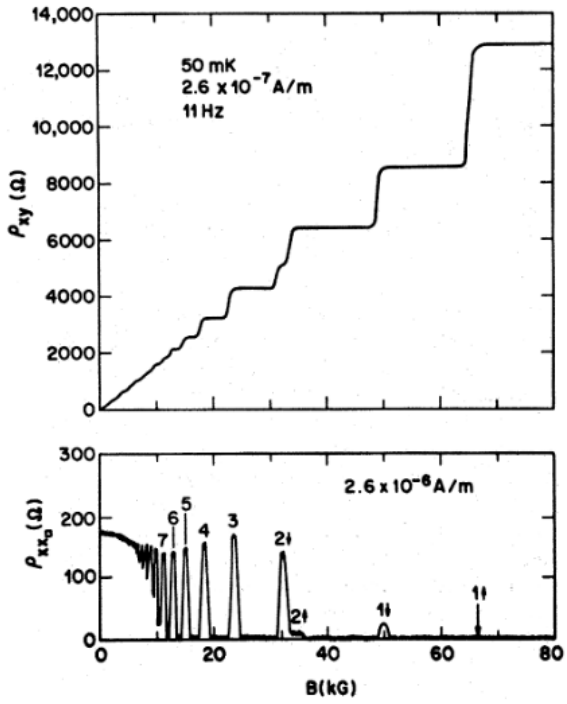

Figure 2.5. *The Hall resistivity and ρ_{xy} the transverse resistivity ρ_{xx}, as functions of the magnetic field strength B. The transverse resistivity forms discrete plateaus with the longitudal resistivity forming spikes at the transition points. [11]*

2.2.2 Edge modes

Topological insulators are classified by their conducting surface states. In two dimensions, these correspond to edge modes at the boundaries of systems with different Chern numbers [12]. The Hamiltonian of a free two-dimensional Dirac fermion is

$$H = k_x\sigma_x + k_y\sigma_y + m\sigma_z, \tag{2.35}$$

where m is the mass of the particle. This system is only gapless when the mass term is equal to zero. As a result, the Chern number may change only when the mass parameter m in equation changes sign.

Let us consider a semi-infinite system with a boundary at $y = 0$. The mass is now a function of y and changes sign at the boundary:

$$\begin{cases} m(y) < 0, & y < 0 \\ m(y) > 0, & y > 0. \end{cases} \tag{2.36}$$

The Hamiltonian can now be written as

$$H(y) = k_x\sigma_x + k_y\sigma_y + m(y)\sigma_z = -\mathrm{i}\partial_x\sigma_x - \mathrm{i}\partial_y\sigma_y + m(y)\sigma_z, \tag{2.37}$$

by using the relation between the $\boldsymbol{k}$-vector and the momentum operator

$$\boldsymbol{k} = \frac{\boldsymbol{p}}{\hbar} = \frac{1}{\hbar}\frac{\hbar}{\mathrm{i}}\nabla = -\mathrm{i}\nabla. \tag{2.38}$$

The wave function is assumed to be separable in the x and y directions

$$\psi(x,y) = \phi(x)\chi(y). \tag{2.39}$$

In the y-direction, the wave function is assumed to of exponential form. This leads to the ansatz

$$\psi(x,y) = \begin{pmatrix}\phi_1(x)\\ \phi_2(x)\end{pmatrix}\mathrm{e}^{-\lambda y}, \tag{2.40}$$

where $\phi(x)$ is a two-component spinor. Thus the Pauli matrices only act on $\phi(x)$ and $\chi(y)$ commutes with any of them. Plugging this into the Schrödinger equation gives the matrix equation

$$\begin{aligned} H\phi(x)\chi(y) &= \begin{pmatrix} m(y) & -\mathrm{i}\partial_x + \mathrm{i}\partial_y \\ -\mathrm{i}\partial_x - \mathrm{i}\partial_y & -m(y)\end{pmatrix}\begin{pmatrix}\phi_1(x)\\ \phi_2(x)\end{pmatrix}\mathrm{e}^{-\lambda y} \\ &= \begin{pmatrix} m(y) & k_x - \mathrm{i}\lambda \\ k_x + \mathrm{i}\lambda & -m(y)\end{pmatrix}\begin{pmatrix}\phi_1(x)\\ \phi_2(x)\end{pmatrix}\mathrm{e}^{-\lambda y} \\ &= E\phi(x)\chi(y), \end{aligned} \tag{2.41}$$

wher E is the energy eigenvalue. Solving the characteristic equation leads to two solutions for the parameter

$$\lambda = \pm\sqrt{m^2(y) - k_x^2 - E^2}, \tag{2.42}$$

corresponding to positive and negative values of y. The wave function decays exponentially when moving away from the border, as seen in Figure 2.6. Writing the Schrödinger equation in terms of the Pauli matrices and separating the variables leads to

$$\begin{aligned} H\psi(x,y) &= E\psi(x,y) \\ -\mathrm{i}\chi(y)\partial_x\sigma_x\phi(x) - \mathrm{i}\partial_y\chi(y)\sigma_y\phi(x) + m(y)\chi(y)\sigma_z\phi(x) &= E\phi(x)\chi(y) \\ -\mathrm{i}\partial_x\sigma_x\phi(x) - \frac{\mathrm{i}}{\chi(y)}\partial_y\chi(y)\sigma_y\phi(x) + m(y)\sigma_z\phi(x) &= E\phi(x) \\ -\mathrm{i}\partial_x\sigma_x\phi(x) - m(y)(\mathrm{i}\sigma_y\phi(x) + \sigma_z\phi(x)) &= E\phi(x). \end{aligned} \tag{2.43}$$

To have a zero energy mode at $k_x = 0$, the second term on the left hand side must be

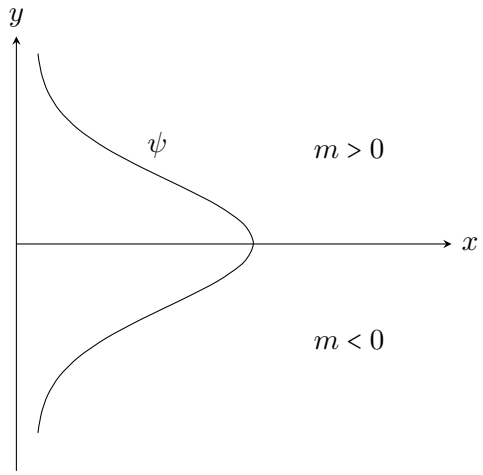

Figure 2.6. *Boundary of two Dirac Hamiltonians with different mass signs. The edge mode ψ decays exponentially for positive and negative values of y.*

zero:

$$\begin{aligned} \mathrm{i}\sigma_y\phi(x) + \sigma_z\phi(x) &= 0 \\ \mathrm{i}\sigma_y\phi(x) &= -\sigma_z\phi(x) \\ \mathrm{i}\sigma_z\sigma_y\phi(x) &= -\sigma_z^2\phi(x) \\ \sigma_x\phi(x) &= -\phi(x). \end{aligned} \tag{2.44}$$

So $\phi(x)$ is an eigenstate of the σ_x operator. Plugging this back into the Schrödinger equation gives

$$\mathrm{i}\partial_x\phi(x) = E\phi(x) = k_x\phi(x), \tag{2.45}$$

where the energy dispersion is linear in k_x. The solution to this is

$$\phi(x) = \frac{1}{\sqrt{2}}\begin{pmatrix} 1 \\ -1 \end{pmatrix}\mathrm{e}^{\mathrm{i}k_x x}, \tag{2.46}$$

which is a right propagating edge mode. This is called a chiral edge mode, where the chirality refers to the fact that there are only electrons moving in one direction on the edge. In the opposite edge the electrons move in the opposite direction.

A Chern insulator may have any number of right or left propagating edge modes. However, the difference between the number of right moving and left moving edge modes is determined by the topological properties of the bulk. The relationship between the bulk structure and the topological edge modes is characterized by the bulk-boundary correspondence

$$N_R - N_L = \Delta n, \tag{2.47}$$

where N_R and N_L are the number of right and left moving edge modes and Δn the difference in Chern number between either side of the edge. [13]

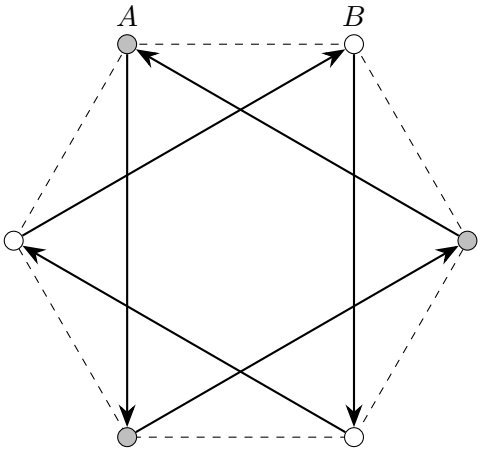

Figure 2.7. *The next-nearest neighbor hoppings in the Haldane model. The hopping is* $+\mathrm{i}t_2$ *in the direction of the arrow and* $-\mathrm{i}t_2$ *in the opposite direction.*

2.2.3 Haldane model

The Haldane model describes a Chern insulator on a honeycomb lattice and is one of the simplest models for a topological insulator. The Haldane model Hamiltonian [14] in the position basis is

$$H = t_1 \sum_{\langle ij \rangle} c_i^\dagger c_j + \mathrm{i}t_2 \sum_{\langle\langle ij \rangle\rangle} \nu_{ij} c_i^\dagger c_j + M \sum_i \epsilon_i c_i^\dagger c_i, \tag{2.48}$$

where $\langle\langle ij \rangle\rangle$ are the next-nearest neighbors. These couplings are between either two A sites or two B sites. The sign of the phase ν_{ij} is calculated as

$$\nu_{ij} = (\boldsymbol{d}_i \times \boldsymbol{d}_j) \cdot \hat{\boldsymbol{z}}, \tag{2.49}$$

where the vectors d_i and d_j are along the two bonds leading to the next-nearest neighbor site. These are shown explicitly in Figure 2.7. The parameters t_1 and t_2 determine the strength of the nearest and next-nearest neighbor hoppings, respectively. The term ϵ_i equals 1 for A sites and -1 for B sites. The creation operators $c_i^\dagger$ now range over both sites in the unit cell.

The Haldane model adds additional terms to the graphene Hamiltonian given in equation 2.21. The sublattice symmetry of the system is broken by sites A and B having different on-site energies. Assigning the energy to differ only by sign gives a term proportional to the σ_z matrix in the Fourier transformed Hamiltonian. This type of perturbation corresponds to adding mass to the Dirac fermion which opens up the band gap. The TR symmetry is broken by adding a term corresponding to the hopping between nearest-neighbor sites. The hopping parameter is imaginary, so there is also a phase change.

Let us perform the Fourier transform given in equation 2.14. The first term is identical to the one in the simplified graphene model and transforms into the familiar form

$$t_1(\cos(\boldsymbol{k} \cdot \boldsymbol{a}_1) + \cos(\boldsymbol{k} \cdot \boldsymbol{a}_2) + 1)\sigma_x + t_1(\sin(\boldsymbol{k} \cdot \boldsymbol{a}_1) + \sin(\boldsymbol{k} \cdot \boldsymbol{a}_2))\sigma_y. \tag{2.50}$$

The last term can be straightforwardly evaluated to be

$$M\sigma_z. \tag{2.51}$$

The second term is not quite so straightforward. The next-nearest-neighbor vectors corresponding to positive hoppings are given in terms of the lattice vectors as

$$\boldsymbol{\delta'} = \boldsymbol{a}_1,\ -\boldsymbol{a}_2,\ \boldsymbol{a}_2 - \boldsymbol{a}_1. \tag{2.52}$$

The vectors giving the negative hoppings are simply the negations. Writing the second term in the Hamiltonian in terms of these gives

$$\mathrm{i}t_2 \sum_{j,\boldsymbol{\delta'}} c_j^\dagger c_{j+\boldsymbol{\delta'}} - c_{j+\boldsymbol{\delta'}}^\dagger c_j \tag{2.53}$$

where $\boldsymbol{\delta'}$ ranges over the next-nearest-neighbor vectors and j over all the sites. Substituting the Fourier transformed operator 2.14 turns this into

$$\mathrm{i}t_2 \sum_{j,\boldsymbol{\delta'}} \sin\big(\boldsymbol{k}\cdot\boldsymbol{\delta'}\big) c_{\boldsymbol{k}}^\dagger c_{\boldsymbol{k}}. \tag{2.54}$$

Overall, this gives the Hamiltonian written in the form given by equation 2.26 as

$$\begin{aligned} d_0 &= 0 \\ d_1 &= t_1(\cos(\boldsymbol{k}\cdot\boldsymbol{a}_1) + \cos(\boldsymbol{k}\cdot\boldsymbol{a}_2) + 1) \\ d_2 &= t_1(\sin(\boldsymbol{k}\cdot\boldsymbol{a}_1) + \sin(\boldsymbol{k}\cdot\boldsymbol{a}_2)) \\ d_3 &= M + 2t_2(\sin(\boldsymbol{k}\cdot\boldsymbol{a}_1) - \sin(\boldsymbol{k}\cdot\boldsymbol{a}_2) - \sin(\boldsymbol{k}\cdot(\boldsymbol{a}_1 - \boldsymbol{a}_2)) \end{aligned} \tag{2.55}$$

Unlike the simple graphene model, there is a term proportional to the σ_z matrix. This means that for some values of M and t_2, the band gap may open up or close allowing a quantum phase transition between a trivial and a topological phase. Let us expand this Hamiltonian around the two TR invariant points of the honeycomb lattice. The expansion around $\boldsymbol{K}$ is

$$h(\boldsymbol{K} + \delta\boldsymbol{k}) \approx \frac{3}{2}t_1(\delta k_x\sigma_x - \delta k_y\sigma_y) + (M - 3\sqrt{3}t_2)\sigma_z. \tag{2.56}$$

The gap closes at $M = 3\sqrt{3}t_2$. Expanding around $\boldsymbol{K'}$ yields

$$h(\boldsymbol{K'} + \delta\boldsymbol{k}) \approx -\frac{3}{2}t_1(\delta k_x\sigma_x + \delta k_y\sigma_y) + (M + 3\sqrt{3}t_2)\sigma_z, \tag{2.57}$$

where the gap closes at $M = -3\sqrt{3}t_2$. So for certain values of t_2, one of the gaps closes but the other remains open.

The closing of the gap leads to chiral edge modes meaning that the system has entered a topological phase. The Dirac cones which form on the $\boldsymbol{K}$ and $\boldsymbol{K'}$ points are the sources of the Berry curvature. When t_2 is near zero, the contributions have opposite signs, leading to a Chern number of zero and trivial phase. When $t_2 > \frac{M}{3\sqrt{3}}$, the gap at $\boldsymbol{K}$ closes

changing the sign of the Dirac cone from -1 to +1. This leads to a Chern number of +1. Similarly, when $t_2 < -\frac{M}{3\sqrt{3}}$, the Dirac cone at $\boldsymbol{K}'$ changes its sign leading to a Chern number of -1. [15]

2.2.4 Kane-Mele Model

Now it is time to restore the electron spin, which has been ignored in the models thus far. The Kane-Mele model is a generalization of the Haldane model for spinful fermions. It was the first model of a topological insulator with TR symmetry preserved. This required a new topological invariant to classify the phase, called the $\mathbb{Z}_2$ invariant.

The model effectively consists of two copies of the Haldane model, one for spin up and one for spin down electrons. The full Hamiltonian is written as

$$H = t\sum_{\langle ij\rangle} c_i^\dagger c_j + \mathrm{i}\lambda_{SO}\sum_{\langle\langle ij\rangle\rangle} \nu_{ij} c_i^\dagger \sigma_z c_j + \mathrm{i}\lambda_R \sum_{\langle ij\rangle} c_i^\dagger (\boldsymbol{\sigma}\times \boldsymbol{d}_{ij})_z c_j + \lambda_v \sum_i \epsilon_i c_i^\dagger c_i, \tag{2.58}$$

where σ_z is the Pauli Z matrix, $\boldsymbol{\sigma}$ the Pauli vector and $\boldsymbol{d}_{ij}$ the vector from site i to site j. The strengths of the nearest-neighbor hopping, spin-orbit coupling, the Rashba effect and the inversion symmetry violating term are described by t, λ_{SO}, λ_R and λ_v, respectively. The phases ν_{ij} are the same as in the Haldane model, as given in Figure 2.7.

Compared to the Haldane model, the next-nearest-neighbor hopping term is replaced by a spin-orbit coupling term. An additional term is also added for nearest-neighbors, which describes the Rashba effect. This term breaks the symmetry in the z-direction.

Once again, we shall perform the Fourier transform as given in equation 2.14. Now that there are two sites with both spin-up and spin-down states, the basis is four-dimensional. The Bloch Hamiltonian may be written in terms of the Dirac gamma matrices $\gamma = \tau \otimes \sigma$, where σ represents the spin degree of freedom for the electrons. The first term is symmetric with regards to spin, so the spin part is just proportional to identity. To write the Hamiltonian in terms of the gamma matrices, a representation must first be explicitly chosen. However, the chosen representation does not affect the properties of the system. We may, for example choose

$$\gamma_{1,2,3,4,5} = \begin{pmatrix} \tau_x & \tau_z & \tau_y\sigma_x & \tau_y\sigma_y & \tau_y\sigma_z \end{pmatrix} \tag{2.59}$$

or any other mutually anticommuting set. The first term of the Hamiltonian is similar to the nearest-neighbor hopping term of the Haldane model, so from equation 2.50 we have

$$t_1(\cos(\boldsymbol{k}\cdot\boldsymbol{a}_1) + \cos(\boldsymbol{k}\cdot\boldsymbol{a}_2) + 1)\gamma_1 - t_1(\sin(\boldsymbol{k}\cdot\boldsymbol{a}_1) + \sin(\boldsymbol{k}\cdot\boldsymbol{a}_2))\gamma_{12}. \tag{2.60}$$

Let us perform the coordinate change

$$x = \frac{a}{2}k_x, \quad y = \frac{\sqrt{3}a}{2}k_y. \tag{2.61}$$

d_1	$t(1+2\cos x\cos y)$	d_{12}	$-2t\cos x\sin y$
d_2	λ_ν	d_{15}	$\lambda_{SO}(2\sin 2x-4\sin x\cos y)$
d_3	$\lambda_R(1-\cos x\cos y)$	d_{23}	$-\lambda_R\cos x\sin y$
d_4	$-\sqrt{3}\lambda_R\sin x\sin y$	d_{24}	$\sqrt{3}\lambda_R\sin x\cos y,$

Table 2.1. *Coefficients for the Kane-Mele Model.*

This has the effect of changing the above expression into

$$t_1(\cos(y-x)+\cos(y+x)+1)\gamma_1-2t_1\cos x\cos y\gamma_{12}. \tag{2.62}$$

The second transforms into

$$2\lambda_{SO}-(2\sin(2x)-4\sin x\cos y)\gamma_{15} \tag{2.63}$$

and so on. All of the coefficients of the gamma matrices are given in Table 2.1 [16]. Setting the Rashba term to zero ($\lambda_R = 0$), the Hamiltonian can be split into two parts, corresponding to spin up and spin down states. For each of these parts, the Chern number may be determined separately. For $\lambda_R \neq 0$, the Chern numbers can not be defined, so the $\mathbb{Z}_2$ index is needed to classify the phase of the system.

2.2.5 Time reversal and inversion symmetries

The time reversal operator T reverses the arrow of time:

$$T : t \to -t. \tag{2.64}$$

This does not mean it reverses the time-evolution of the system, but rather it reverses the motion of each particle in the system. If a system has time reversal (TR) symmetry, the particles will trace back their paths exactly. The TR symmetry may be broken by an external magnetic field or by some other symmetry-breaking mechanism. The operator can generally be written as

$$T = UK, \tag{2.65}$$

where U is a unitary operation and K is the complex-conjugation operation. It is thus an anti-unitary operation satisfying either

$$T^2 = \pm I. \tag{2.66}$$

Given some particle with position $\boldsymbol{r}$ and momentum $\boldsymbol{p}$, the time reversal operator has the following effect:

$$T\boldsymbol{r}T^{-1} = \boldsymbol{r}, \quad T\boldsymbol{p}T^{-1} = -\boldsymbol{p}. \tag{2.67}$$

So the position remains unchanged, but the momentum gets its sign flipped. In other

words, the position is even and the momentum odd under the TR operation. Since the crystal momentum $\boldsymbol{k}$ is a momentum, its sign is also flipped under the operation

$$T\boldsymbol{k}T^{-1} = -\boldsymbol{k}. \tag{2.68}$$

This means that for a system to have TR symmetry the Hamiltonian must satisfy $H(-\boldsymbol{k}) = H(\boldsymbol{k})$.

If the particle is spinless, the time reversal operator squares to identity

$$T^2 = I. \tag{2.69}$$

Adding spin makes things more interesting. The spin of a particle is odd under TR

$$T\boldsymbol{S}T^{-1} = -\boldsymbol{S}. \tag{2.70}$$

For particles with integer spin, the system acts as before. However, for particles with half-integer spin, we have

$$T^2 = -I. \tag{2.71}$$

If the Hamiltonian of the system has an eigenstate $|n\rangle$ and commutes with the time-reversal operator

$$[H, T] = 0, \tag{2.72}$$

then the state $T|n\rangle$ is also an eigenstate of the Hamiltonian with the same eigenenergy. For fermionic systems this time-reversed state is not equal to the original state. This leads to Kramer's theorem: if the system has half-integer total spin, each energy eigenstate is at least doubly degenerate.

The inversion operator P flips the direction of the spatial coordinates. For a particle with position $\boldsymbol{r}$ and momentum $\boldsymbol{p}$ the operator flips their signs

$$P\boldsymbol{r}P^{-1} = -\boldsymbol{r}, \quad P\boldsymbol{p}P^{-1} = -\boldsymbol{p}. \tag{2.73}$$

The crystal momentum $\boldsymbol{k}$ is similarly affected by the operation

$$P\boldsymbol{k}P^{-1} = -\boldsymbol{k}. \tag{2.74}$$

These symmetries are important tools in determining the general properties of systems, as well as classifying the different topological insulators.

3 TWO-BAND SYSTEMS

3.1 General Hamiltonian

The most general form for the Hamiltonian of a two-band system is a 2×2 Hermitian matrix. Any such matrix can be written as a linear combination of the identity matrix and the three Pauli matrices. The Pauli matrices satisfy the commutation relations

$$\{\sigma_i, \sigma_j\} = 2\delta_{ij}, \quad [\sigma_i, \sigma_j] = 2\mathrm{i}\varepsilon_{ijk}\sigma_k, \tag{3.1}$$

where ε is the Levi-Civita symbol. These form a Clifford algebra known as the Pauli algebra.

The Hamiltonian is then given by

$$H = d_0 I + d_1\sigma_x + d_2\sigma_y + d_3\sigma_z = d_0 I + \boldsymbol{d}\cdot\boldsymbol{\sigma}, \tag{3.2}$$

where $\boldsymbol{\sigma}$ is the vector of Pauli matrices. The coefficients d_0, d_1, d_2 and d_3 are some real-valued functions of $\boldsymbol{k}$ periodic in the Brillouin zone. The eigenvalues of this Hamiltonian are

$$E_\pm = d_0 \pm d, \tag{3.3}$$

where $d = \sqrt{d_1^2 + d_2^2 + d_3^2}$. Since the term proportional to the identity has only the effect of shifting the eigenvalues, it can be ignored without changing the topological properties of the system. The resulting Hamiltonian

$$H = \boldsymbol{d}(\boldsymbol{k})\cdot\boldsymbol{\sigma} \tag{3.4}$$

can be used to model a two-dimensional Dirac fermion, where d_3 is the mass term. If this term is zero, the band structure is gapless. If it is some constant m, the band structure is gapped. If the energy dispersion around such a point where the gap closes is linear, it is called a Dirac point. In Chern insulators, the closing and opening of the gap is what allows the phase transitions. This means that d_3 must be a function of some parameter of the Hamiltonian, for example the strength of an external magnetic field. By tuning this parameter, the phase of the system may be controlled.

3.2 Chern number

The Chern number of a Chern insulator is related to a gauge-invariant quantity called the Berry curvature. The Berry curvature is a consequence of the phase change the system undergoes during an adiabatic process. This phase change is called the geometric phase, or Berry phase. [17]

Start with a Hamiltonian, which is a function of some parameters $\boldsymbol{R}$. The eigenstates of this system are given by the time-independent Schrödinger equation

$$H(\boldsymbol{R})\,|n(\boldsymbol{R})\rangle = E_n(\boldsymbol{R})\,|n(\boldsymbol{R})\rangle\,, \tag{3.5}$$

where E_n is the energy of state n. The eigenstates form a complete basis of the Hilbert space. Let the system initially be in an eigenstate of the Hamiltonian. Then vary the parameters $\boldsymbol{R}$ slowly along some path in the parameter space as a function of time t. If the process is done adiabatically, the system remains in the same eigenstate of the Hamiltonian up to a phase $\theta(t)$. The full state of the system during this process is

$$|\psi(t)\rangle = \mathrm{e}^{-\mathrm{i}\theta(t)}\,|n(\boldsymbol{R}(t)\rangle\,. \tag{3.6}$$

The time evolution of this state is given by the time-dependent Schrödinger equation

$$H(\boldsymbol{R}(t))\,|\psi(t)\rangle = \mathrm{i}\hbar\frac{\mathrm{d}}{\mathrm{d}t}\,|\psi(t)\rangle\,, \tag{3.7}$$

where $\hbar$ is the reduced Planck constant. Inserting the state from equation 3.6 into this equation and solving the resulting differential equation gives the solution for the phase

$$\theta(t) = \frac{1}{\hbar}\int_0^t E_n(\boldsymbol{R}(t'))\,\mathrm{d}t' - \mathrm{i}\int_0^t \left\langle n(\boldsymbol{R}(t'))\middle|\frac{\mathrm{d}}{\mathrm{d}t'}\middle|n(\boldsymbol{R}(t'))\right\rangle \mathrm{d}t'\,. \tag{3.8}$$

The first part of this equation is the dynamic phase, which can be cancelled by a suitable gauge transformation. This gauge-dependence means it can not correspond to any physical observable. The negative of the second term is called the Berry phase [18]. If the path taken by the parameters in some (long) time T forms a closed loop such that $R(T) = R(0)$, the Berry phase has no explicit time dependence. This means it can be written as

$$\gamma_n = \mathrm{i}\int_0^T \langle n(\boldsymbol{R}(t'))|\nabla_{\boldsymbol{R}}|n(\boldsymbol{R}(t'))\rangle\,\frac{\mathrm{d}\boldsymbol{R}}{\mathrm{d}t'}\,\mathrm{d}t' = \mathrm{i}\oint_{\mathcal{C}} \langle n(\boldsymbol{R})|\nabla_{\boldsymbol{R}}|n(\boldsymbol{R})\rangle\,\mathrm{d}\boldsymbol{R}\,, \tag{3.9}$$

where $\mathcal{C}$ is the path in the parameter space. Since this form has no time-dependence, only the path taken matters. The integrand of this equation

$$\boldsymbol{A}_n = \mathrm{i}\,\langle n(\boldsymbol{R})|\nabla|n(\boldsymbol{R})\rangle \tag{3.10}$$

is called the Berry connection. The parameter space is assumed to be three-dimensional for notational simplicity. According to Stokes' theorem, the line integral of a vector function along a closed path is equal to the surface integral of its curl over the surface enclosed by the path. By applying this result here, the Berry phase can also be calculated as

$$\gamma_n = \oint_{\mathcal{C}} \boldsymbol{A}_n \cdot \mathrm{d}\boldsymbol{R} = \iint_S (\nabla \times \boldsymbol{A}_n) \cdot \mathrm{d}\boldsymbol{S}\,, \tag{3.11}$$

where S is the surface enclosed by the path. To get the Berry connection of the full system, it is summed over all the filled energy bands

$$\boldsymbol{A} = \sum_{n\,\text{filled}} \boldsymbol{A}_n = \mathrm{i} \sum_{n\,\text{filled}} \langle n(\boldsymbol{R}) | \nabla | n(\boldsymbol{R}) \rangle\,. \tag{3.12}$$

This corresponds to all the bands up to the Fermi level, which for insulators lies in the band gap.

Taking the curl of the Berry connection gives the vector field $\boldsymbol{F} = \nabla \times \boldsymbol{A}$. This field can be thought of as analogous to a magnetic field in the parameter space. The accompanying magnetic vector potential is then the Berry connection $\boldsymbol{A}$. For this reason, $\boldsymbol{A}$ is also known as the Berry vector potential. The integral of the magnetic field over a surface give the total magnetic flux through the surface. For an actual magnetic field the integral over a closed surface is zero since there are no magnetic monopoles. For this reason, the magnetic flux is not quantized. For the Berry curvature, the integral over a closed surface gives some integer multiple of 2π. This is due to Chern's theorem, which is a generalization of the Gauss-Bonnet theorem relating the geometry of an object to its topology. The integer factor is a topological invariant called the Chern number.

For an insulator, the surface S is the full Brillouin zone. Dividing the integral of $\boldsymbol{F}$ over the BZ with 2π gives the Chern number. For a two dimensional system in the (k_x, k_y) plane only the z-component of $\boldsymbol{F}$ contributes to the integral, denoted as F_{xy}. From this follows the formula

$$c = \frac{1}{2\pi} \iint_{\mathrm{BZ}} F_{xy}(\boldsymbol{k})\, \mathrm{d}k_x\, \mathrm{d}k_y\,, \tag{3.13}$$

where the quantity

$$F_{xy}(\boldsymbol{k}) = (\nabla \times \boldsymbol{A}) \cdot \hat{\boldsymbol{z}} = \frac{\partial A_y}{\partial k_x} - \frac{\partial A_x}{\partial k_y} \tag{3.14}$$

is called the Berry curvature of the system. Unlike the Berry phase and the Berry connection, this quantity can be shown to be gauge invariant. According to Stokes' theorem, the Chern number could also be calculated via the line integral along the boundary. Since the BZ is topologically a torus it has no boundary and the Chern number would be always zero. However, this only holds for smooth and continuous function meaning that the Berry connection must have singularities inside the BZ. The number of these singularities is equal to the Chern number. These singularities must exist no matter the chosen gauge.

The Hall conductance σ_{xy} of the system is obtained by multiplying the Chern number

by the fundamental quantum e^2/h. The quantization of the Hall conductance is thus a consequence of the topology of the band structure. Impurities in the material can not change the topological properties of the system. The effect can thus be measured even in impure samples.

If the system is described by the 2D Dirac Hamiltonian given in equation 3.4, the Berry curvature can also be written in the convenient form [19]

$$F_{xy}(\boldsymbol{k}) = \frac{1}{2d^3}\epsilon_{abc} d_a \partial_x d_b \partial_y d_c, \tag{3.15}$$

which uses the Einstein summation convention, where the indices a, b, c range from 1 to 3. The Levi-Civita symbol ϵ_{abc} satisfies

$$\epsilon_{abc} = \begin{cases} 1 & \text{for even permutations of (1, 2, 3)} \\ -1 & \text{for odd permutations of (1, 2, 3)} \\ 0 & \text{otherwise,} \end{cases} \tag{3.16}$$

which gives three positive and three negative terms to the expression for Berry curvature. From this form it can be clearly seen that if one of the components of $\boldsymbol{d}$ is zero, the Berry curvature is trivially zero and therefore the Chern number as well. This is assuming that $\boldsymbol{d}$ is also smooth and continuous.

3.3 Spin rotations

The state of the Hamiltonian given in equation 3.4 is defined by the three-dimensional vector $\boldsymbol{d}$. This vector can be rotated by applying the spin-rotation operator

$$U(\hat{\boldsymbol{n}}, \phi) = \mathrm{e}^{-\mathrm{i}\frac{\phi}{2}\hat{\boldsymbol{n}}\cdot\boldsymbol{\sigma}}, \tag{3.17}$$

which corresponds to a counterclockwise rotation around the axis $\hat{\boldsymbol{n}}$ by ϕ. Such a transformation has the following effect on the Hamiltonian and the state:

$$\widetilde{H} = UHU^\dagger, \quad |\tilde{\psi}\rangle = U|\psi\rangle, \tag{3.18}$$

where the transformed quantities are marked with a tilde. Since this rotation is unitary ($UU^\dagger = U^\dagger U = I$), it preserves the eigenvalues of the Hamiltonian. Knowing the transformation, it is also easy to solve the eigenvectors in one coordinate system and then transform it into the other. The rotation operator can also be written as

$$U(\hat{\boldsymbol{n}}, \phi) = \cos\frac{\phi}{2} I - \mathrm{i}\sin\frac{\phi}{2}\hat{\boldsymbol{n}}\cdot\boldsymbol{\sigma}, \tag{3.19}$$

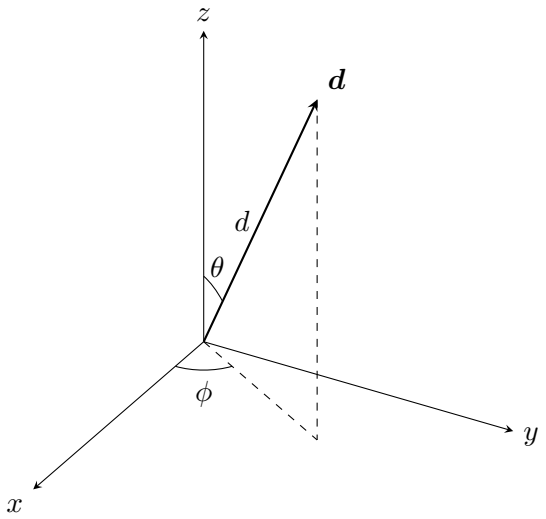

Figure 3.1. *Vector $\boldsymbol{d}$ written in spherical coordinates, where d is the radial distance, θ the polar angle and ϕ the azimuthal angle.*

since $\hat{\boldsymbol{n}} \cdot \boldsymbol{\sigma}$ is involutory (squares to identity). The vector $\boldsymbol{d}$ can also be written in spherical coordinates as

$$\boldsymbol{d} = d \begin{pmatrix} \sin\theta\cos\phi \\ \sin\theta\sin\phi \\ \cos\theta \end{pmatrix}, \tag{3.20}$$

where d is the radial distance, θ the polar angle and ϕ the azimuthal angle. This is shown in Figure 3.1.

3.4 Term elimination

Start with the Hamiltonian given in equation 3.4 with the eigenstate

$$H\left|\psi\right\rangle = -d\left|\psi\right\rangle, \tag{3.21}$$

which corresponds to the lower energy band. The Fermi energy lies in the band gap, so only this band is occupied which lets us ignore the upper band. We want to eliminate one of the terms in the Hamiltonian with a suitable rotation. This is achieved by rotating the vector $\boldsymbol{d}$ in a plane until it is aligned with one of the axes. The rotation axis $\hat{\boldsymbol{n}}$ is then the axis orthogonal to this plane. Since the rotation axis is aligned with one of the coordinate axes, it has only component. This simplifies equation 3.17 into

$$U = \mathrm{e}^{\mathrm{i}\frac{\phi}{2}\sigma}, \tag{3.22}$$

where σ is some Pauli matrix. The suitable angle of rotation is of the form

$$\phi = \arctan\frac{f(\boldsymbol{k})}{g(\boldsymbol{k})}, \tag{3.23}$$

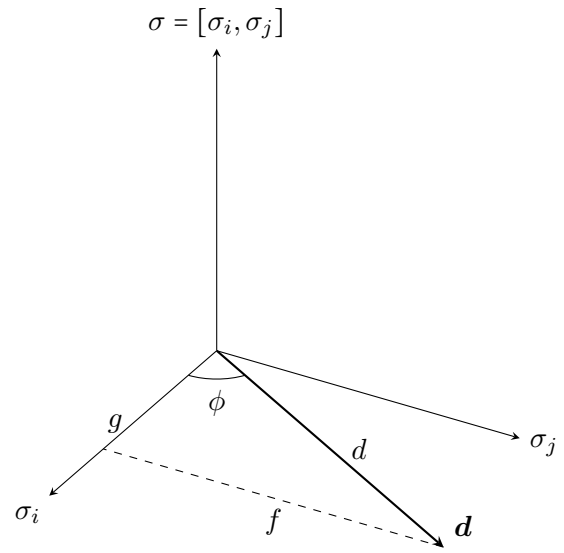

Figure 3.2. *Rotation around axis σ. For clarity the term proportional to σ is zero since it is not affected by the rotation.*

where f is the factor of the term to be eliminated and g is the factor of the other term in the rotation plane. The rotation plane is shown in Figure 3.2. The Berry connection can be calculated from equation 3.12 as

$$\boldsymbol{A} = \mathrm{i} \langle \psi | \nabla | \psi \rangle , \tag{3.24}$$

where the sum has been reduced to only term. Applying U to this state, the Berry connection transforms into

$$\begin{aligned} \widetilde{\boldsymbol{A}} &= \mathrm{i} \langle \psi | U^\dagger \nabla (U | \psi \rangle) \\ &= \mathrm{i} \langle \psi | U^\dagger \left(U \nabla | \psi \rangle + \nabla U | \psi \rangle \right) \\ &= \mathrm{i} \langle \psi | U^\dagger U \nabla | \psi \rangle + \mathrm{i} \langle \psi | U^\dagger \nabla U | \psi \rangle \\ &= \mathrm{i} \langle \psi | \nabla | \psi \rangle + \mathrm{i} \langle \psi | U^\dagger U \frac{\mathrm{i}}{2} \sigma \nabla \phi | \psi \rangle \\ &= \boldsymbol{A} - \frac{1}{2} \langle \psi | \sigma | \psi \rangle \nabla \phi. \end{aligned} \tag{3.25}$$

The first term is just the original Berry connection. The second term is given by the expectation value of the Pauli matrix and the gradient of the rotation angle. The expectation value is calculated in the original state so it acts as a constant. The gradient, however, is dependent on $\boldsymbol{k}$. The transformed Berry curvature is the curl of this function

$$\begin{aligned} \widetilde{\boldsymbol{F}} &= \nabla \times \boldsymbol{A} - \frac{1}{2} \langle \psi | \sigma | \psi \rangle \nabla \times \nabla \phi \\ &= \boldsymbol{F} - \frac{1}{2} \langle \psi | \sigma | \psi \rangle \nabla \times \nabla \phi. \end{aligned} \tag{3.26}$$

Now the transformed Berry curvature could also be calculated with equation 3.15. As mentioned in the previous section, since one component of $\boldsymbol{d}$ has been eliminated, the whole equation evaluates to zero. Since $\widetilde{\boldsymbol{F}}$ is zero, the untransformed Berry curvature

can be solved from the previous equation to be

$$\boldsymbol{F} = \frac{1}{2} \langle \psi | \sigma | \psi \rangle \nabla \times \nabla \phi. \tag{3.27}$$

This expression contains the curl of the gradient of a function. For any continuous smooth function, this would be zero. Since we know that the answer is not zero, the function cannot be analytic in the whole region. Calculating the gradient of ϕ gives

$$\nabla \phi = \frac{g \nabla f - f \nabla g}{f^2 + g^2}, \tag{3.28}$$

which has a singularity whenever $f = g = 0$. Everywhere else in the BZ, the function is defined. This means that the integral of the Berry curvature over the BZ reduces to just integrating over the singularities. By using Stokes' theorem, these can be evaluated via path integrals around the singularities. The path can be made arbitrarily small, so the function can be substituted by a first order approximation. The Taylor expansion of a function $f(\boldsymbol{k})$ around a singularity $\boldsymbol{k}^*$ is

$$\begin{aligned} f(\boldsymbol{k}) &= f(\boldsymbol{k}^*) + (\boldsymbol{k} - \boldsymbol{k}^*) \cdot \nabla f(\boldsymbol{k}^*) + (\boldsymbol{k} - \boldsymbol{k}^*)^2 \cdot \nabla^2 f(\boldsymbol{k}^*) + \cdots \\ &\approx (\boldsymbol{k} - \boldsymbol{k}^*) \cdot \nabla f(\boldsymbol{k}^*), \end{aligned} \tag{3.29}$$

giving us the first order approximation. By performing the coordinate change $\boldsymbol{k} - \boldsymbol{k}^* \to \boldsymbol{k}$ and introducing the notation $\boldsymbol{u} = \nabla f(\boldsymbol{k}^*)$ and $\boldsymbol{v} = \nabla g(\boldsymbol{k}^*)$, the functions can be simplified to

$$\begin{aligned} f(\boldsymbol{k}) &\approx \boldsymbol{k} \cdot \boldsymbol{u} = k_x u_x + k_y u_y \\ g(\boldsymbol{k}) &\approx \boldsymbol{k} \cdot \boldsymbol{v} = k_x v_x + k_y v_y. \end{aligned} \tag{3.30}$$

These can be substituted into the gradient of the rotation angle given in equation 3.28. With some algebraic manipulation this turns into

$$\begin{aligned} \nabla \phi &= \frac{(\boldsymbol{k} \cdot \boldsymbol{v})\boldsymbol{u} - (\boldsymbol{k} \cdot \boldsymbol{u})\boldsymbol{v}}{(\boldsymbol{k} \cdot \boldsymbol{u})^2 + (\boldsymbol{k} \cdot \boldsymbol{v})^2} \\ &= \frac{1}{(\boldsymbol{k} \cdot \boldsymbol{u})^2 + (\boldsymbol{k} \cdot \boldsymbol{v})^2} \begin{pmatrix} \cancel{k_x v_x u_x} + k_y v_y u_x - \cancel{k_x u_x v_x} - k_y u_y v_x \\ -k_x v_x u_y - \cancel{k_y v_y u_y} + k_x u_x v_y + \cancel{k_y u_y v_y} \\ 0 \end{pmatrix} \\ &= \frac{u_x v_y - u_y v_x}{(\boldsymbol{k} \cdot \boldsymbol{u})^2 + (\boldsymbol{k} \cdot \boldsymbol{v})^2} \begin{pmatrix} k_y \\ -k_x \\ 0 \end{pmatrix} \\ &= \frac{1}{k} \frac{u_x v_y - u_y v_x}{(u_x \cos\theta + u_y \sin\theta)^2 + (v_x \cos\theta + v_y \sin\theta)^2} \begin{pmatrix} \sin\theta \\ -\cos\theta \\ 0 \end{pmatrix} \end{aligned} \tag{3.31}$$

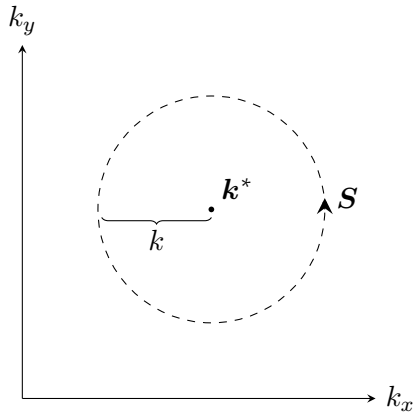

Figure 3.3. *Path $\boldsymbol{S}$ around the singularity $\boldsymbol{k}^*$. The path is circular with radius k.*

Stokes' theorem gives the relation between the integral of the curl of a function over an area and the path integral around the area

$$\iint_A \nabla \times \nabla\phi \cdot \mathrm{d}\boldsymbol{A} = \oint_S \nabla\phi \cdot \mathrm{d}\boldsymbol{S}\,, \tag{3.32}$$

where A is the integration area and $\boldsymbol{S}$ the path around its edge in the counter-clockwise direction. The circular path in the (k_x, k_y) plane around zero can be parametrized as

$$\boldsymbol{S} = k \begin{pmatrix} \cos\theta \\ \sin\theta \\ 0 \end{pmatrix}, \tag{3.33}$$

where k is some constant radius and the angle $\theta \in [0, 2\pi)$. This path is shown in Figure 3.3. This gives the differential line element

$$\mathrm{d}\boldsymbol{S} = k\,\mathrm{d}\theta \begin{pmatrix} -\sin\theta \\ \cos\theta \\ 0 \end{pmatrix}. \tag{3.34}$$

Equations 3.31 and 3.34 can now be substituted into the right hand side of equation 3.32. The path being proportional to k and the function being inversely proportional to k cancel each other out leaving an expression that is only a function of the angle θ. This is easily integrated around a full circle as

$$\begin{aligned} \oint_S \nabla\phi \cdot \mathrm{d}\boldsymbol{S} &= (u_x v_y - u_y v_x) \int_0^{2\pi} \frac{-\sin^2\theta - \cos^2\theta}{(u_x\cos\theta + u_y\sin\theta)^2 + (v_x\cos\theta + v_y\sin\theta)^2}\,\mathrm{d}\theta \\ &= -(u_x v_y - u_y v_x)\frac{1}{|u_x v_y - u_y v_x|} \\ &= 2\pi\,\mathrm{sign}(u_y v_x - u_x v_y) \\ &= 2\pi\,\mathrm{sign}((\nabla g(\boldsymbol{k}^*) \times \nabla f(\boldsymbol{k}^*)) \cdot \hat{\boldsymbol{z}}). \end{aligned} \tag{3.35}$$

Each singularity contributes a factor of 2π with the sign determined by the values of the functions f and g at the singularity. This means that $\nabla \times \nabla\phi$ acts like the Dirac delta function centered at the singularity

$$\nabla \times \nabla\phi = \operatorname{sign}(u_y v_x - u_x v_y) 2\pi\delta(f^2 + g^2). \tag{3.36}$$

The expectation value of σ can be calculated as

$$\langle\psi|\sigma|\psi\rangle = \langle\psi|U^\dagger U\sigma|\psi\rangle = \langle\psi|U^\dagger\sigma U|\psi\rangle = \langle\tilde{\psi}|\sigma|\tilde{\psi}\rangle \tag{3.37}$$

since U commutes with σ. This means that it may be calculated either in the original or the transformed basis. Furthermore, the expectation value of an operator may be calculated without needing to first calculate the eigenvectors by using the relation

$$\langle\psi|\sigma|\psi\rangle = \operatorname{Tr}\big(\sigma P_\psi\big), \tag{3.38}$$

where Tr denotes matrix trace and P_ψ is the projection operator onto state ψ. The projection operator can be obtained by calculating the Frobenius covariant

$$P_i = \prod_{i\neq j} \frac{H - E_j}{E_i - E_j} \tag{3.39}$$

for a Matrix H with eigenvalues E_i. For a two-dimensional system this gives

$$P_\psi = \frac{1}{2}\left(I - \frac{H}{d}\right). \tag{3.40}$$

Substituting equation 3.35 into the equation for the Chern number given in equation 3.13 and using the above results gives the final equation for the Chern number

$$c = \frac{1}{2}\sum_{\boldsymbol{k}^*} \operatorname{sign}\big((\nabla g \times \nabla f)\cdot\hat{\boldsymbol{z}}\big)\operatorname{Tr}\big(\sigma P_\psi\big), \tag{3.41}$$

where $\boldsymbol{k}^*$ ranges over the singularities. This formula holds when choosing any two components of the $\boldsymbol{d}$ vector as f and g. Then it is just a matter of finding the zeros $f = g = 0$ and performing the sum over those points.

4 FOUR-BAND SYSTEMS

4.1 Dirac matrices

In two dimensions, the three Pauli matrices are enough to satisfy the Clifford algebra of the Dirac equation. The three-dimensional analog of the Pauli matrices are the five Dirac gamma matrices $\gamma_1, \ldots, \gamma_5$. They are 4×4 matrices which satisfy the relations

$$\gamma_\mu^2 = I, \quad \{\gamma_\mu, \gamma_\nu\} = 2\delta_{\mu\nu} I, \tag{4.1}$$

forming the Clifford algebra. They form a complete basis for 4×4 Hermitian matrices together with the identity matrix and the ten commutator matrices defined as

$$\gamma_{\mu\nu} = \frac{1}{2\mathrm{i}}[\gamma_\mu, \gamma_\nu], \tag{4.2}$$

where μ and ν range from 1 to 5. Swapping the indices gives just the negation of the matrix

$$\gamma_{\nu\mu} = -\gamma_{\mu\nu}, \tag{4.3}$$

so these terms need not be included in the basis. The commutator matrices anti-commute with each other if one of the indices matches and commute if none match. They also commute with the Dirac matrices if the index matches one of the indices.

The Dirac matrices are operators of a four-dimensional Hilbert space, which can be divided into two subspaces

$$\mathcal{H} = \mathcal{H}_\tau \otimes \mathcal{H}_\sigma, \tag{4.4}$$

where $\otimes$ is the tensor product. In the Kane and Mele model, for example, τ denotes the sublattice and σ the spin subspace. The subspaces are spanned by the three Pauli matrices and the 2×2 identity matrix. This means that the basis elements of the whole space can be represented as the Kronecker product of two Pauli matrices or a Pauli matrix and the identity matrix

$$\gamma_\mu = \tau \otimes \sigma, \quad \tau, \sigma \in \{I, \sigma_x, \sigma_y, \sigma_z\}. \tag{4.5}$$

Now, any five mutually anticommuting combinations can be chosen as the five Dirac matrices. This means that the exact form of the matrices depends on the chosen representation. For them to be block diagonal, the τ matrix must be equal to identity or σ_z. For

	TR	I
$\boldsymbol{\gamma} = \begin{pmatrix}\gamma_1 & \gamma_2 & \gamma_3\end{pmatrix}$	-1	-1
γ_4	+1	+1
$\gamma_5 = \gamma_1\gamma_2\gamma_3\gamma_4$	+1	+1

Table 4.1. *Symmetry properties of the Dirac gamma matrices.*

any representation, this only holds for at most three of the five Dirac matrices.

4.2 General Hamiltonian

Since the Dirac matrices form a basis for the 4×4 Hermitian matrices, any four-band hamiltonian can be written as a linear combination of them. The general four-band Hamiltonian with TR and I symmetry preserved can be written as

$$H_0 = n(\boldsymbol{k})I + \boldsymbol{\kappa}(\boldsymbol{k})\cdot\boldsymbol{\gamma} + m(\boldsymbol{k})\gamma_4, \tag{4.6}$$

where the coefficients n and m are symmetric real functions with respect to $\boldsymbol{k}$ and the vector $\boldsymbol{\kappa}$ is real and anti-symmetric:

$$n(-\boldsymbol{k}) = n(\boldsymbol{k}), \quad m(-\boldsymbol{k}) = m(\boldsymbol{k}), \quad \boldsymbol{\kappa}(-\boldsymbol{k}) = -\boldsymbol{\kappa}(\boldsymbol{k}). \tag{4.7}$$

This means that to preserve the symmetries of the Hamiltonian, the matrices γ_1, γ_2, γ_3 must be chosen to be odd and γ_4 even under both TR and I. The fifth gamma matrix γ_5 is given as the product of the other four so it must also be even under both symmetry operations. These properties have been collected in Table 4.1. Similarly to the two-band system, the term proportional to identity has only the effect of shifting the eigenvalues, so it can be ignored. This means we are left with the Hamiltonian

$$H_0 = \boldsymbol{\kappa}(\boldsymbol{k})\cdot\boldsymbol{\gamma} + m(\boldsymbol{k})\gamma_4, \tag{4.8}$$

where we have set $n = 0$.

The symmetries of the commutator matrices likewise follow from these symmetry properties. They can be seen to break either the TR or the I symmetry. They can be grouped based on these properties into three sets of mutually anticommuting matrices and one set with only the remaining matrix [20]. These groupings are shown in Table 4.2. The most general four-band Hamiltonian with TR and I breaking (TRIB) fields is thus

$$H = H_0 + \boldsymbol{u}\cdot\boldsymbol{b} + \boldsymbol{w}\cdot\boldsymbol{p} + \boldsymbol{u}'\cdot\boldsymbol{b}' + f\varepsilon, \tag{4.9}$$

where $\boldsymbol{u}$, $\boldsymbol{w}$, $\boldsymbol{u}'$ are real-valued three-dimensional vectors and f is a real valued function. In the systems examined in this thesis, either TR or I symmetry is broken. This means that at least some of the TRIB fields are going to be nonzero in systems of interest.

	TR	I
$\boldsymbol{b} = \begin{pmatrix}\gamma_{23} & \gamma_{31} & \gamma_{12}\end{pmatrix}$	-1	+1
$\boldsymbol{p} = \begin{pmatrix}\gamma_{14} & \gamma_{24} & \gamma_{34}\end{pmatrix}$	+1	-1
$\boldsymbol{b}' = \begin{pmatrix}\gamma_{15} & \gamma_{25} & \gamma_{35}\end{pmatrix}$	-1	+1
$\varepsilon = \gamma_{45}$	+1	-1

Table 4.2. *Symmetry properties of the commutator matrices.*

4.3 Z2 invariant

In Chern insulators, the TR symmetry was necessarily broken. There is another class of topological insulators with intact TR symmetry. The Chern number for such systems is zero. There is another topological invariant corresponding to these systems called the $\mathbb{Z}_2$ invariant. It has only two values corresponding to a topological and a trivial phase. In this thesis, 0 is taken to be the trivial and 1 the topological phase. The $\mathbb{Z}_2$ invariant also generalizes to higher dimensions. If a two-dimensional system has two edges the surface states form a Dirac cone. Near the Dirac cone, the effective mass of the electrons goes to zero.

The $\mathbb{Z}_2$ invariant corresponds to the parity of the number of Kramers pairs localized on the edges of the system. The Fermi arc encloses an odd number of Dirac points. This is not allowed in a conventional conductor due to Kramers degeneracy. In general, calculating the $\mathbb{Z}_2$ invariant for an arbitrary four-band system is more cumbersome than it was for the two-band system. The two-band system could be solved analytically for the most general case, but that is not possible here. There are general algorithms to calculate the $\mathbb{Z}_2$ invariant but they do not lead to an analytical formula. Taking advantage of the underlying symmetries of the system may simplify the calculations. There are several different approaches to calculating the $\mathbb{Z}_2$ invariant, for example:

- Parity of the spin Chern number via adiabatic continuity,
- Integral of the Bloch wave functions,
- Evaluate the zeros of the Pfaffian.

This thesis focuses on the first approach.

If the four-band Hamiltonian is in a block diagonal form, the problem reduces to two uncoupled two-band systems. Then the Hamiltonian is of the form

$$H = \begin{pmatrix} H_+ & 0 \\ 0 & H_- \end{pmatrix} = \begin{pmatrix} \boldsymbol{d}_+ \cdot \boldsymbol{\sigma} & 0 \\ 0 & \boldsymbol{d}_- \cdot \boldsymbol{\sigma} \end{pmatrix}, \tag{4.10}$$

where H_+ and H_- are called the upper and lower blocks, respectively. For each of these blocks, the Chern number can be calculated individually, as before. This results in two surface modes with opposite spin and chirality. These states form a Dirac cone at each

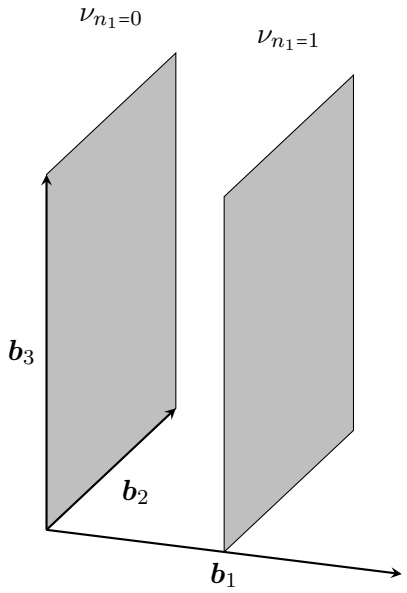

Figure 4.1. *Two slices of a three-dimensional topological insulator separated by half a lattice vector. This leads to 2 two-dimensional systems with their own $\mathbb{Z}_2$ invariants. If they are different, the material is a strong topological insulator.*

surface. Then the $\mathbb{Z}_2$ invariant of the whole four-band system is given by

$$\nu = \frac{c_+ - c_-}{2} \pmod 2, \tag{4.11}$$

where $c_\pm$ are the Chern numbers for the blocks. A value of zero corresponds to a trivial phase and a one to a topological phase. The Chern number of the whole system is just zero. The $\mathbb{Z}_2$ invariant now corresponds to the parity of the spin Chern number.

Unlike the Chern number, the $\mathbb{Z}_2$ invariant generalizes to three dimensions. The Hamiltonian is reduced to two dimensions by fixing one coordinate to a value where the system is TR invariant. These TR invariant planes are displaced from the origin by half a lattice vector. The points in the BZ satisfy

$$\boldsymbol{k} = n_1\frac{\boldsymbol{b}_1}{2} + n_2\frac{\boldsymbol{b}_2}{2} + n_3\frac{\boldsymbol{b}_3}{2}, \quad n_1, n_2, n_3 \in [-1, 1], \tag{4.12}$$

where $\boldsymbol{b}_i$ are the reciprocal lattice vectors. Three weak invariants are obtained this way by setting $n_i = 1$ for some lattice vector and calculating the $\mathbb{Z}_2$ invariant using equation 4.11 in the resulting planar system. A fourth, strong invariant is obtained by taking the difference $\nu_{n_i=1} - \nu_{n_i=0} \pmod 2$ for any i. This result does not depend on the particular lattice vector chosen. This is helpful, since whichever is the most convenient to calculate may be chosen. Figure 4.1 shows one such choice. The strong invariant is labeled as ν_0 and the weak ones $\nu_{1,2,3}$. The $\mathbb{Z}_2$ insulators can be classified by listing all four of the invariants.

4.4 Block diagonalization

The problem now is how to transform a non block diagonal matrix into the block diagonal form. It is straightforward to do numerically, but having an analytical formula would be more convenient. Furthermore, it would allow to determine the properties of the system more easily. Even the symmetry preserving Hamiltonian given in equation 4.8 can not be exactly block diagonalized. Three of the Dirac matrices can be block diagonalized by choosing an appropriate representation, but it is not possible to do this for all four matrices in general. However, by using the rotation operator given in equation 4.15, it is possible to eliminate one of these terms and then choose a representation which turns the Hamiltonian into the desired block diagonal form. It is even possible to add some TRIB fields. If two matrices are block diagonal, then their commutator is also block-diagonal. Using this fact it is possible to figure out which terms can be left in.

If the Hamiltonian has $\boldsymbol{\kappa} \neq 0$ and $m \neq 0$ then all terms with index 5 have to be disgarded for the block diagonalization to work. Since γ_5 can not be chosen to be block-diagonal then neither are any of its commutators. Thus $\boldsymbol{u}'$ and f are set to zero, which leaves the TR breaking term $\boldsymbol{u}$ and the I breaking term $\boldsymbol{w}$ giving the Hamiltonian

$$H = \boldsymbol{\kappa} \cdot \boldsymbol{\gamma} + m\gamma_4 + \boldsymbol{u} \cdot \boldsymbol{b} + \boldsymbol{w} \cdot \boldsymbol{p}. \tag{4.13}$$

In addition to the anticommutation relation, the elements of $\boldsymbol{b}$ satisfy the full Pauli algebra

$$\{b_i, b_j\} = 2\delta_{ij}, \quad [b_i, b_j] = 2\mathrm{i}\varepsilon_{ijk} b_k, \tag{4.14}$$

which means that the operator

$$U = \mathrm{e}^{\mathrm{i}\frac{\phi}{2}\hat{\boldsymbol{n}}\cdot\boldsymbol{b}} \tag{4.15}$$

corresponds to a rotation of ϕ around the axis $\hat{\boldsymbol{n}}$. This has a similar form to the spin rotation in a two-dimensional system. The other vectors may also be written as $\boldsymbol{p} = -\gamma_5 \boldsymbol{b}$, $\boldsymbol{b}' = \gamma_4 \boldsymbol{b}$ and $\boldsymbol{\gamma} = -\gamma_{45} \boldsymbol{b}$. This means that an operator of the same form can be used to rotate any of the other vectors as well. At least two cases can be easily evaluated: systems with only either TR or I breaking. If both symmetries are broken, the analytical calculation for the block diagonalization is in general not possible. [21]

4.4.1 Broken TR symmetry

Let us first focus on the case where the TR symmetry is broken, but the I symmetry remains intact. This corresponds to the case where $\boldsymbol{w} = 0$ and $\boldsymbol{u} \neq 0$, giving the Hamiltonian

$$H = \boldsymbol{\kappa}(\boldsymbol{k}) \cdot \boldsymbol{\gamma} + m(\boldsymbol{k})\gamma_4 + \boldsymbol{u} \cdot \boldsymbol{b}. \tag{4.16}$$

There is no representation for the gamma matrices where this is completely block diagonal. There is a way to transform this into a block diagonalizable form by doing two

rotations. Firstly, we want to align $\boldsymbol{u}$ with the x-axis. This is achieved by applying the rotation

$$U = \mathrm{e}^{\mathrm{i}b_2 \frac{\theta-\pi/2}{2}} \mathrm{e}^{\mathrm{i}b_3 \frac{\phi}{2}} = \mathrm{e}^{\mathrm{i}\gamma_{31} \frac{\theta-\pi/2}{2}} \mathrm{e}^{\mathrm{i}\gamma_{12} \frac{\phi}{2}}, \tag{4.17}$$

where θ and ϕ are the polar and azimuthal angle of $\boldsymbol{u}$, written in spherical coordinates. Applying this transformation to the Hamiltonian results in

$$UHU^\dagger = \boldsymbol{K}(\boldsymbol{k}) \cdot \boldsymbol{\gamma} + m(\boldsymbol{k})\gamma_4 + u\gamma_{23}, \tag{4.18}$$

where the vector

$$\boldsymbol{K} = \begin{pmatrix} \boldsymbol{\kappa} \cdot \hat{\boldsymbol{u}} & \frac{(\hat{\boldsymbol{u}} \times \boldsymbol{\kappa}) \cdot \hat{\boldsymbol{z}}}{\sqrt{1-\hat{u}_3^2}} & \frac{(\hat{\boldsymbol{u}} \times (\boldsymbol{\kappa} \times \hat{\boldsymbol{u}})) \cdot \hat{\boldsymbol{z}}}{\sqrt{1-\hat{u}_3^2}} \end{pmatrix} \tag{4.19}$$

has been introduced. This leaves the γ_{23} term present, which means that the terms γ_2, γ_3, γ_{23} can be chosen to be block diagonal simultaneously. This leaves γ_1 and γ_4, of which only one can be block diagonal. This means that either γ_1 or γ_4 must be eliminated by a subsequent rotation. We choose to eliminate the γ_1 term via the rotation

$$R = \mathrm{e}^{\mathrm{i}\frac{\rho}{2}\gamma_{14}}, \tag{4.20}$$

where the angle is given by

$$\rho = \arctan \frac{K_1}{m}. \tag{4.21}$$

This results in the final form

$$RUHU^\dagger R^\dagger = K_2\gamma_2 + K_3\gamma_3 + m\sqrt{1 + \frac{K_1^2}{m^2}}\gamma_4 + u\gamma_{23}, \tag{4.22}$$

which has only four terms. Now the representation

$$\gamma_{1,2,3,4} = \begin{pmatrix} \tau_x & \tau_z\sigma_x & \tau_z\sigma_y & \tau_z\sigma_z \end{pmatrix} \tag{4.23}$$

can be chosen to arrive at a block Hamiltonian with blocks defined as

$$H_\pm = \pm K_2\sigma_x \pm K_3\sigma_y + \left(u \pm m\sqrt{1 + \frac{K_1^2}{m^2}}\right)\sigma_z, \tag{4.24}$$

where H_+ and H_- are the upper and lower blocks in a 4×4 matrix.

4.4.2 Broken I symmetry

The other case, which can be analytically evaluated is with I symmetry broken but TR symmetry preserved. This corresponds to $\boldsymbol{u} = 0$ and $\boldsymbol{w} \neq 0$, giving the Hamiltonian

$$H = \boldsymbol{\kappa} \cdot \boldsymbol{\gamma} + m\gamma_4 + \boldsymbol{w} \cdot \boldsymbol{p}. \tag{4.25}$$

Since $\boldsymbol{p} = -\gamma_5 \boldsymbol{b}$ and γ_5 commutes with U, the transformation given in equation 4.17 can be used to the same effect as in the case with the broken TR symmetry. The transformed Hamiltonian is then

$$UHU^\dagger = \boldsymbol{K} \cdot \boldsymbol{\gamma} + m\gamma_4 + w\gamma_{14}, \tag{4.26}$$

where the vector $\boldsymbol{K}$ is identical to the one given equation 4.19, except with $\boldsymbol{u}$ replaced with $\boldsymbol{w}$:

$$\boldsymbol{K} = \begin{pmatrix} \boldsymbol{\kappa} \cdot \hat{\boldsymbol{w}} & \frac{(\hat{\boldsymbol{w}} \times \boldsymbol{\kappa}) \cdot \hat{\boldsymbol{z}}}{\sqrt{1-\hat{w}_3^2}} & \frac{(\hat{\boldsymbol{w}} \times (\boldsymbol{\kappa} \times \hat{\boldsymbol{w}})) \cdot \hat{\boldsymbol{z}}}{\sqrt{1-\hat{w}_3^2}} \end{pmatrix}. \tag{4.27}$$

Now either the γ_2 or the γ_3 term must be eliminated to fully block diagonalize the Hamiltonian. We choose to eliminate γ_3 by applying the rotation

$$R = \mathrm{e}^{\mathrm{i}\frac{\nu}{2}\gamma_{23}} \tag{4.28}$$

where the angle is once again of the form

$$\nu = \arctan \frac{K_3}{K_2}. \tag{4.29}$$

This results in the rotated Hamiltonian

$$RUHU^\dagger R^\dagger = K_1\gamma_1 + K_2\sqrt{1 + \frac{K_3^2}{K_2^2}}\gamma_2 + m\gamma_4 + w\gamma_{14}. \tag{4.30}$$

Choosing the representation

$$\gamma_{1,2,3,4} = \begin{pmatrix} \tau_z\sigma_x & \tau_z\sigma_z & \tau_x & \tau_z\sigma_y \end{pmatrix} \tag{4.31}$$

the blocks are

$$H_\pm = \pm K_1\sigma_x \pm m\sigma_y + \left(w \pm K_2\sqrt{1 + \frac{K_3^2}{K_2^2}} \right)\sigma_z, \tag{4.32}$$

where H_+ is once again the upper and H_- the lower block.

4.5 Bismuth selenide

Now let us examine the bismuth selenide (Bi_2Se_3) family of three-dimensional $\mathbb{Z}_2$ insulators on a cubic lattice. It has three weak $\mathbb{Z}_2$ invariants and one strong invariant given by the formula 4.11. This family of topological insulators is described by the Hamiltonian [22]

$$H_0 = 2\lambda(\sin k_x\gamma_1 + \sin k_y\gamma_2) + 2\lambda_z \sin k_z\gamma_3 + M_{\boldsymbol{k}}\gamma_4, \tag{4.33}$$

where

$$M_{\boldsymbol{k}} = \mu - 2t\sum_{\alpha=1}^{3} \cos k_\alpha. \tag{4.34}$$

This is known to have a topological phase for values $\lambda, \lambda_z > 0$ and $2t < \mu < 6t$. Setting any of the coordinates to 0 or π leaves only three terms remaining which can all be chosen to be block diagonal with a suitable representation.

We are interested in how the properties of the system are affected by an I-breaking term. We can assume that it is aligned with the x-axis since the more general case with the full $\boldsymbol{w}$ vector is no more difficult to handle. The more general case was seen to reduce to this form in section 4.4.2. The full Hamiltonian is then

$$H = H_0 + w\gamma_{14}. \tag{4.35}$$

To calculate the strong $\mathbb{Z}_2$ invariant the system can be split into planes in any direction. If we choose k_y or k_z for the direction the Hamiltonian can again be trivially block diagonalized in the suitable representation. For example, choosing $k_z = 0, \pi$ gives

$$H = 2\lambda(\sin k_x\gamma_1 + \sin k_y\gamma_2) + M_{\boldsymbol{k}}\gamma_4 + w\gamma_{14}. \tag{4.36}$$

Now the representation

$$\gamma_{1,2,3,4} = \begin{pmatrix} \tau_z\sigma_x & \tau_z\sigma_z & \tau_x & \tau_z\sigma_y \end{pmatrix} \tag{4.37}$$

gives a block diagonal matrix with blocks

$$H_\pm = \pm 2\lambda \sin k_x\sigma_x \pm M_{\boldsymbol{k}}\sigma_y + (|w| \pm 2\lambda \sin k_y)\sigma_z. \tag{4.38}$$

This works similarly in the k_y direction.

However, the k_x direction presents a problem. The resulting Hamiltonian has terms γ_2, γ_3, γ_4 and γ_{14}, only three of which can simultaneously be block diagonal. Let us eliminate the γ_3 term with a rotation, as before. Using the same representation as above, the matrix has blocks

$$H_\pm = \pm M_{\boldsymbol{k}}\sigma_y + \left(|w| + 2\lambda \sin k_y \sqrt{1 + \left(\frac{\lambda_z \sin k_z}{\lambda \sin k_y} \right)^2} \right) \sigma_z. \tag{4.39}$$

The Chern number is trivially zero for both blocks since the σ_x term is absent. This is not in agreement with the other directions. This is especially troubling since we know that setting $w = 0$ should give us a topological phase for some values of the parameters.

This can be remedied by performing an additional rotation on the full Hamiltonian to turn the $\boldsymbol{w}$ from pointing in the x-direction to pointing in the y-direction. This operation is simply a quarter-turn around the z-axis. The rotation operator is then

$$U = \mathrm{e}^{-\mathrm{i}\frac{\pi}{4}b_3} = \mathrm{e}^{-\mathrm{i}\frac{\pi}{4}\gamma_{12}}. \tag{4.40}$$

This operations only affects the γ_1 and γ_2 terms in addition to turning the $\boldsymbol{w}$ vector. The

full transformed Hamiltonian is then

$$UHU^{\dagger} = \frac{1}{\sqrt{2}}(\kappa_1 - \kappa_2)\gamma_1 + \frac{1}{\sqrt{2}}(\kappa_1 + \kappa_2)\gamma_2 + \kappa_3\gamma_3 + m\gamma_4 + w\gamma_{24}. \tag{4.41}$$

Now setting $\kappa_1 = 0$ leads to

$$UHU^{\dagger} = -\frac{1}{\sqrt{2}}\kappa_2\gamma_1 + \frac{1}{\sqrt{2}}\kappa_2\gamma_2 + \kappa_3\gamma_3 + m\gamma_4 + w\gamma_{24}. \tag{4.42}$$

Now using the method outlined in section 4.4.2 leads to the blocks

$$H_{\pm} = \mp\frac{1}{\sqrt{2}}\kappa_2\sigma_x \pm m\sigma_y + \left(|w| \pm \frac{1}{\sqrt{2}}K_2\sqrt{1 + \frac{K_3^2}{K_2^2}}\right)\sigma_z \tag{4.43}$$

with well-defined Berry curvature and $\mathbb{Z}_2$ invariants.

5 RESULTS

5.1 Kane-Mele Model

The Kane-Mele model was introduced in section 2.2.4. It is a two-dimensional $\mathbb{Z}_2$ insulator meaning the system has only one topological invariant of interest, the $\mathbb{Z}_2$ index. The Hamiltonian is of the form

$$H = d_1\gamma_1 + d_2\gamma_2 + d_3\gamma_3 + d_4\gamma_4 + d_{12}\gamma_{12} + d_{15}\gamma_{15} + d_{23}\gamma_{23} + d_{24}\gamma_{24}, \tag{5.1}$$

in the representation

$$\gamma_{1,2,3,4,5} = \begin{pmatrix} \tau_x & \tau_z & \tau_y\sigma_x & \tau_y\sigma_y & \tau_y\sigma_z \end{pmatrix}, \tag{5.2}$$

where the gamma matrices are even and their commutators odd under TR. The coefficients d_i were given in Table 2.1. The Rashba term is ignored by setting $\lambda_R = 0$ resulting in the coefficients d_3, d_4, d_{23} and d_{24} being zero. The resulting Hamiltonian is

$$H = d_1\tau_x + d_2\tau_z - d_{12}\tau_y + d_{15}\tau_z\sigma_z, \tag{5.3}$$

given in terms of the Pauli matrices. The coefficients d_1 and d_2 are even under TR with d_{12} and d_{15} being odd. In our representation $\gamma_{1,2,3}$ are odd and γ_4 even so to preserve the TR symmetry of the Hamiltonian γ_4 must be equal to either τ_x or τ_z. The terms τ_y and $\tau_z\sigma_z$ can be chosen to be any two matrices in $\gamma_{1,2,3}$. We choose the representation

$$\gamma_1 = \tau_y, \quad \gamma_2 = \tau_z\sigma_z, \quad \gamma_4 = \tau_x \tag{5.4}$$

which gives the Hamiltonian

$$H = -d_{12}\gamma_1 + d_{15}\gamma_2 + d_1\gamma_4 - d_2\gamma_{14}. \tag{5.5}$$

Applying the block diagonalization procedure described in section 4.4.2 gives the upper and lower blocks as

$$H_\pm = \mp d_{12}\sigma_x \pm (d_2 + d_{15})\sigma_y \pm d_1\sigma_z. \tag{5.6}$$

The spin-orbit coupling term λ_{SO} was set to t and the strength of the inversion symmetry breaking term λ_v was varied from -10 to 10. The $\mathbb{Z}_2$ invariant ν was calculated for each value of the parameter, as shown in Figure 5.1. The system can be seen to be in the

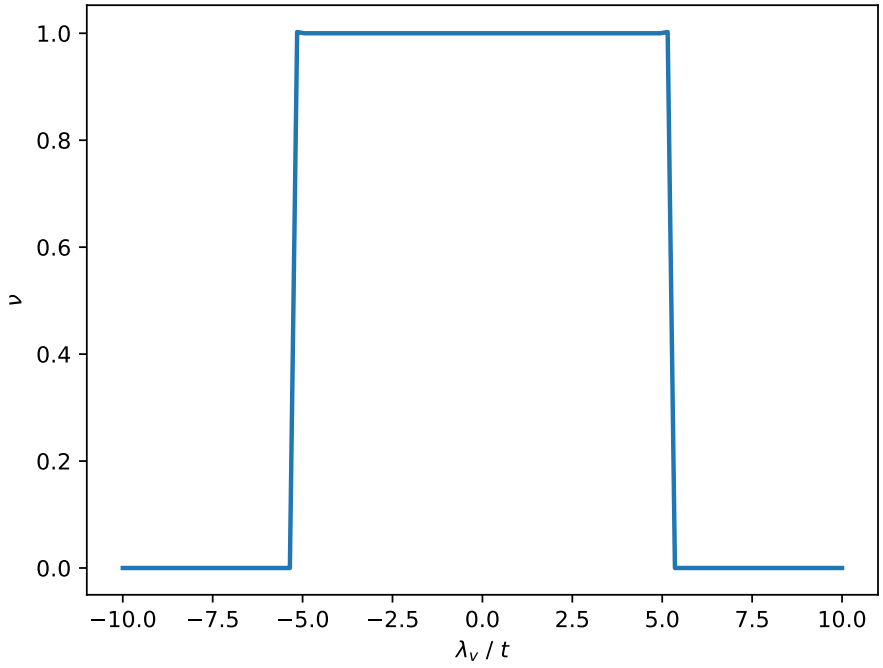

Figure 5.1. *The $\mathbb{Z}_2$ invariant ν for the Kane-Mele model with $\lambda_R = 0$ and $\lambda_{SO} = t$. It is shown as a function of the strength of the inversion-symmetry breaking term λ_v.*

topologically nontrivial phase for values $-5t < \lambda_v < 5t$. At points $\lambda_v = \pm 5t$ the system undergoes a quantum phase transition. For values $\lambda_v > 5t$ and $\lambda_v < -5t$ the system is in the trivial phase.

5.2 Bismuth selenide

This model was introduced in section 4.5 with the Hamiltonian

$$H = 2\lambda(\sin k_x\gamma_1 + \sin k_y\gamma_2) + 2\lambda_z \sin k_z\gamma_3 + (\mu - 2t\sum_{\alpha=1}^{3}\cos k_\alpha)\gamma_4 + w\gamma_{14}, \tag{5.7}$$

with the added I-breaking term proportional to w. Let us set $\lambda = t$ then fix either μ or w to some constant value and vary the other one. For each value, the strong $\mathbb{Z}_2$invariant was calculated. The results are shown in Figure 5.2. Setting $w = t$ and varying μ, this system has a topological phase roughly when $2t < \mu < 6t$. Alternatively setting $\mu = 4t$ and varying w there is a topological phase when $-1.5t < w < 1.5t$.

The original unperturbed system given in equation 4.33 is known to be in the topologically nontrivial phase for values $2t < \mu < 6t$. We saw that a small perturbation, where $|w| < 2$, does not change the topological properties of the system.

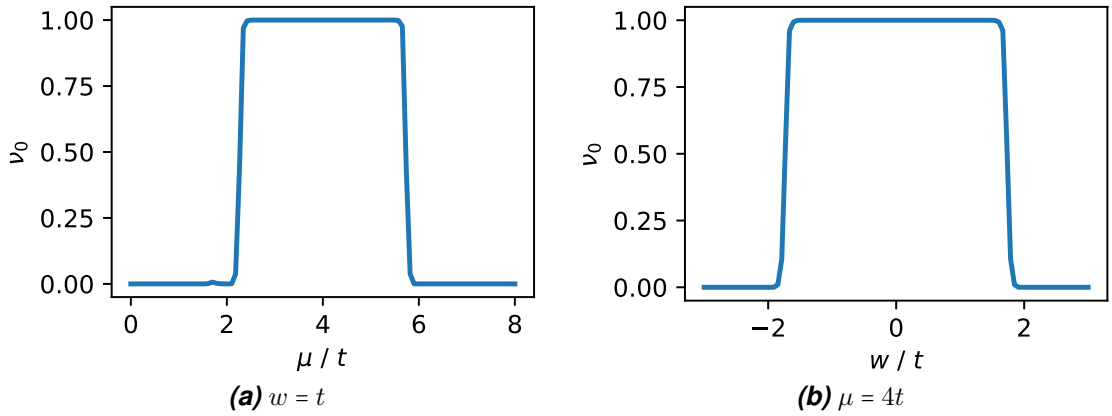

(a) $w = t$ **(b)** $\mu = 4t$

Figure 5.2. *The strong $\mathbb{Z}_2$ invariant ν_0 for the cubic lattice model with $\lambda = t$.*

5.3 Diamond lattice

The diamond lattice is a face-centered cubic (FCC) lattice with a two atom basis separated by $\boldsymbol{d} = \frac{a}{4}\begin{pmatrix}1 & 1 & 1\end{pmatrix}$, where a is the lattice constant. The lattice vectors are

$$\boldsymbol{a}_1 = a\begin{pmatrix}0\\1\\1\end{pmatrix}, \quad a\begin{pmatrix}1\\0\\1\end{pmatrix}, \quad a\begin{pmatrix}1\\1\\0\end{pmatrix}, \tag{5.8}$$

giving the reciprocal lattice vectors

$$\boldsymbol{b}_1 = \frac{2\pi}{a}\begin{pmatrix}-1\\1\\1\end{pmatrix}, \quad \boldsymbol{b}_2 = \frac{2\pi}{a}\begin{pmatrix}1\\-1\\1\end{pmatrix}, \quad \boldsymbol{b}_3 = \frac{2\pi}{a}\begin{pmatrix}1\\1\\-1\end{pmatrix}. \tag{5.9}$$

It is helpful to perform a change of variables to $x = \boldsymbol{k}\cdot\boldsymbol{a}_1$, $y = \boldsymbol{k}\cdot\boldsymbol{a}_2$ and $z = \boldsymbol{k}\cdot\boldsymbol{a}_3$. This makes the integral easier to evaluate since the BZ is simply a cube with side length 2π.

$$\int_{\mathrm{BZ}} \mathrm{d}\boldsymbol{k} = \int_{-\pi}^{\pi}\int_{-\pi}^{\pi}\int_{-\pi}^{\pi} \mathrm{d}x\,\mathrm{d}y\,\mathrm{d}z \tag{5.10}$$

The Hamiltonian can now be written as

$$H = d_1\gamma_1 + d_2\gamma_2 + d_3\gamma_3 + d_4\gamma_4 + d_5\gamma_5, \tag{5.11}$$

where the coefficients d_i are given in Table 5.1 [23]. In this representation γ_1 is even and $\gamma_{2,3,4,5}$ are odd. This Hamiltonian has too many terms to be analytically block diagonalized. This means we have to neglect some of the terms. The spin-orbit coupling terms d_3, d_4, d_5 are identical except for the coordinates, which are permuted cyclically. For this reason, it can be argued that two of them can be ignored without destroying the complex-

d_1	$t + \delta t_1 + t(\cos x + \cos y + \cos z)$
d_2	$t(\sin x + \sin y + \sin z)$
d_3	$\lambda_{SO}(\sin y - \sin z - \sin(y-x) + \sin(z-x))$
d_4	$\lambda_{SO}(\sin z - \sin x - \sin(z-y) + \sin(x-y))$
d_5	$\lambda_{SO}(\sin x - \sin y - \sin(x-z) + \sin(y-z))$

Table 5.1. *Coefficients for the diamond model as functions of* $x = \boldsymbol{k}\cdot\boldsymbol{a}_1, y = \boldsymbol{k}\cdot\boldsymbol{a}_2, z = \boldsymbol{k}\cdot\boldsymbol{a}_3$.

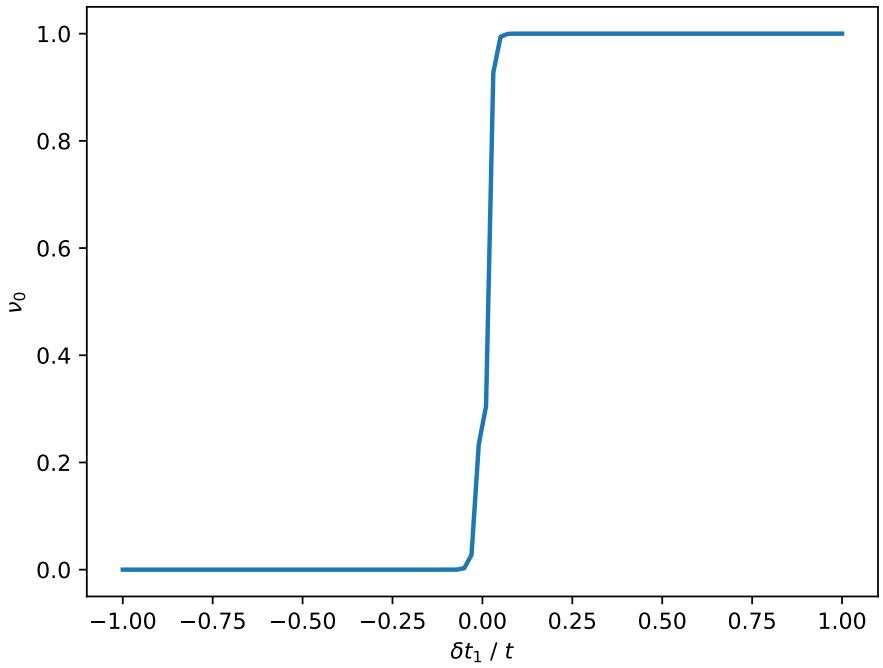

Figure 5.3. *Strong* $\mathbb{Z}_2$ *invariant for the diamond model.*

ity of the system. The terms d_4 and d_5 were thus set to zero. Using our convention for the gamma matrices the Hamiltonian is

$$H = d_2\gamma_1 + d_3\gamma_2 + d_1\gamma_4. \tag{5.12}$$

This Hamiltonian can be made block diagonal by choosing the representation

$$\gamma_{1,2,3,4,5} = \begin{pmatrix} \tau_x & \tau_z & \tau_y\sigma_x & \tau_y\sigma_y & \tau_y\sigma_z \end{pmatrix}. \tag{5.13}$$

Then there is a trivial phase when $\delta t_1 < 0$ and a topological phase when $\delta t_1 > 0$, as shown in Figure 5.3.

d_0	$\frac{1}{2}(\epsilon_s + \epsilon_p) - (t_{ss} - t_{pp})(\cos x + \cos y)$
d_1	$\frac{1}{2}(\epsilon_s - \epsilon_p) - (t_{ss} + t_{pp})(\cos x + \cos y)$
d_2	$2t_{sp} \sin x$
d_5	$2t_{sp} \sin y$

Table 5.2. *Coefficients for the BHZ model.*

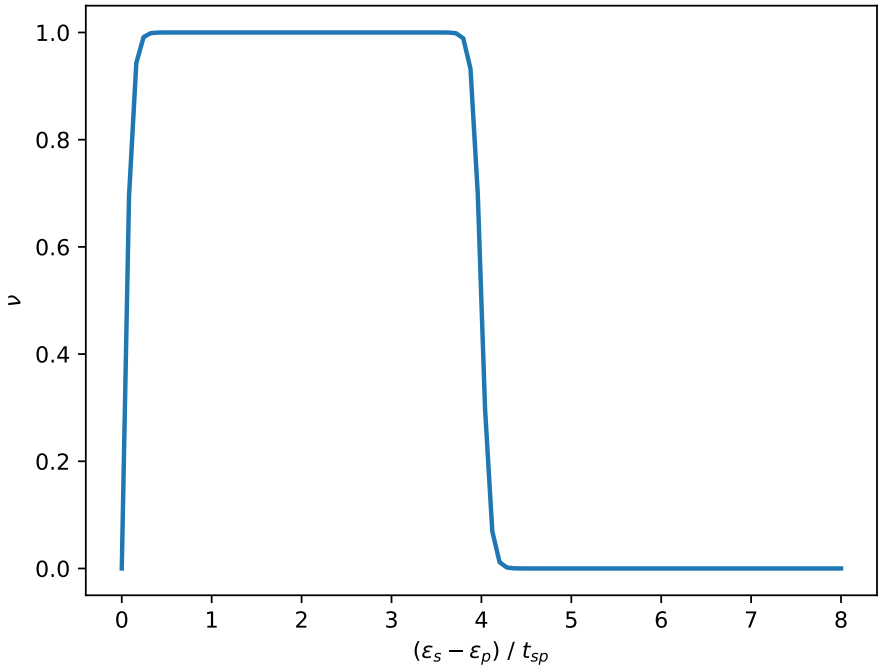

Figure 5.4. *$\mathbb{Z}_2$ invariant for the BHZ model.*

5.4 Bernevig Hughes Zhang Model

The Bernevig Hughes Zhang (BHZ) model describes a system where a layer of HgTe is between CdTe crystals [24]. This is a two-dimensional system on a square lattice. The Hamiltonian is of the form

$$H = d_0 I + d_1\gamma_1 + d_2\gamma_2 + d_5\gamma_5, \tag{5.14}$$

where the coefficients d_i are given in Table 5.2 [25]. The term proportional to identity can be ignored like we have done so far since it does not fundamentally change the behavior of the system. This leaves only three terms remaining. By choosing the representation

$$\gamma_{1,2,3,4,5} = \begin{pmatrix} \tau_z\sigma_x & \tau_z\sigma_y & \tau_x & \tau_z\sigma_z \end{pmatrix} \tag{5.15}$$

the Hamiltonian can be easily block diagonalized. Setting $t_{ss} + t_{pp} = t_{sp}$ there is a topological phase when $\epsilon_s - \epsilon_p < 4t_{sp}$, as shown in Figure 5.4.

6 CONCLUSIONS

The main goal of this thesis was deriving analytical formulas for calculating topological invariants. This included Chern numbers for two-band systems as well as $\mathbb{Z}_2$ invariants for four-band systems. The Chern number is only valid for two-dimensional systems, but the $\mathbb{Z}_2$ invariant generalizes to three dimensions as well. Then there are three weak invariants corresponding to each basis vector of the reciprocal lattice and a strong invariant which can be calculated in any of the three directions.

The two-band Chern insulators are described by a 2×2 Hamiltonian, which can be written as a linear combination of the 3 Pauli matrices and the identity matrix. The general integral formula for calculating the Chern number was presented. It was also shown how the Chern number can be recovered even when a rotation is performed on the system, where one of the terms vanishes. In this case, the integral over the Brillouin zone was reduced to a sum over the singularities of a function.

The four-band $\mathbb{Z}_2$ insulators are described by a 4×4 Hamiltonian. This can be written as a linear combination of the 5 Dirac gamma matrices, their 10 commutators and the identity matrix. The goal was to turn this into a block diagonal form, whereby it reduced to two uncoupled Chern insulators. A topological state then corresponded to differing Chern numbers for these blocks. The block diagonalization is possible to do analytically in the cases were there are only either TR or I symmetry breaking terms. A similar problem to the one in the two-band systems arose in the case of the Bi_2Se_3 insulator with an I breaking term. Calculating the strong $\mathbb{Z}_2$ invariant gave the right answer in two directions but not in the third, where one term was missing from the two-band block Hamiltonians after performing the block diagonalization. This was corrected by performing an additional rotation to restore the missing term.

These results were applied to some example systems. The $\mathbb{Z}_2$ invariant was calculated as a function of some parameter of the Hamiltonian, where a quantum phase transition could be seen. The systems examined were, the Kane-Mele model, bismuth selenide, diamond and the Bernevig Hughes Zhange model.

The results matched with known values from literature. For each model a topological phase emerged with some values of the parameters. These phase changes were accompanied by a discontinuous jump in the graphs, corresponding to integer values for the topological invariants.

The results of this thesis can be used to study the topological properties of other interest-

ing models.

REFERENCES

[1] K. v. Klitzing, G. Dorda and M. Pepper. New Method for High-Accuracy Determination of the Fine-Structure Constant Based on Quantized Hall Resistance. *Phys. Rev. Lett.* 45 (6 Aug. 1980), 494–497. DOI: 10.1103/PhysRevLett.45.494. URL: https://link.aps.org/doi/10.1103/PhysRevLett.45.494.

[2] *The Nobel Prize in Physics 1985. NobelPrize.org*. Jan. 3, 2020. URL: https://www.nobelprize.org/prizes/physics/1985/summary/ (visited on 01/07/2020).

[3] D. B. Newell. A more fundamental International System of Units. *Physics Today* 67.7 (2014), 35–41. DOI: 10.1063/PT.3.2448. eprint: https://doi.org/10.1063/PT.3.2448. URL: https://doi.org/10.1063/PT.3.2448.

[4] H. Zhang, C.-X. Liu, X.-L. Qi, X. Dai, Z. Fang and S.-C. Zhang. *Topological Insulators at Room Temperature*. 2008. arXiv: 0812.1622 [cond-mat.mes-hall].

[5] C. Kane and J. Moore. Topological insulators. *Physics World* 24.02 (Feb. 2011), 32–36. DOI: 10.1088/2058-7058/24/02/36. URL: https://doi.org/10.1088%2F2058-7058%2F24%2F02%2F36.

[6] N. Xu, Y. Xu and J. Zhu. Topological insulators for thermoelectrics. *npj Quantum Materials* 2.1 (Sept. 2017), 51. ISSN: 2397-4648. DOI: 10.1038/s41535-017-0054-3. URL: https://doi.org/10.1038/s41535-017-0054-3.

[7] C. Yue, S. Jiang, H. Zhu, L. Chen, Q. Sun and D. Zhang. Device Applications of Synthetic Topological Insulator Nanostructures. *Electronics* 7.10 (Oct. 2018), 225. ISSN: 2079-9292. DOI: 10.3390/electronics7100225. URL: http://dx.doi.org/10.3390/electronics7100225.

[8] S. D. Sarma, M. Freedman and C. Nayak. Topological quantum computation. *Physics Today* 59.7 (2006), 32–38. DOI: 10.1063/1.2337825. eprint: https://doi.org/10.1063/1.2337825. URL: https://doi.org/10.1063/1.2337825.

[9] H. Bruus and K. Flensberg. *Many-body quantum theory in condensed matter physics: an introduction*. Oxford university press, 2004.

[10] Y. Yao, F. Ye, X.-L. Qi, S.-C. Zhang and Z. Fang. Spin-orbit gap of graphene: First-principles calculations. *Physical Review B* 75.4 (Jan. 2007). ISSN: 1550-235X. DOI: 10.1103/physrevb.75.041401. URL: http://dx.doi.org/10.1103/PhysRevB.75.041401.

[11] M. A. Paalanen, D. C. Tsui and A. C. Gossard. Quantized Hall effect at low temperatures. *Phys. Rev. B* 25 (8 Apr. 1982), 5566–5569. DOI: 10.1103/PhysRevB.25.5566. URL: https://link.aps.org/doi/10.1103/PhysRevB.25.5566.

[12] B. A. Bernevig and T. L. Hughes. *Topological insulators and topological superconductors*. Princeton university press, 2013.

[13] M. Z. Hasan and C. L. Kane. Colloquium: Topological insulators. *Rev. Mod. Phys.* 82 (4 Nov. 2010), 3045–3067. DOI: 10.1103/RevModPhys.82.3045. URL: https://link.aps.org/doi/10.1103/RevModPhys.82.3045.

[14] F. D. M. Haldane. Model for a Quantum Hall Effect without Landau Levels: Condensed-Matter Realization of the "Parity Anomaly". *Phys. Rev. Lett.* 61 (18 Oct. 1988), 2015–2018. DOI: 10.1103/PhysRevLett.61.2015. URL: https://link.aps.org/doi/10.1103/PhysRevLett.61.2015.

[15] T. Delft and course contributors. *Topology in Condensed Matter*. 2019. URL: https://topocondmat.org/ (visited on 01/09/2019).

[16] C. L. Kane and E. J. Mele. Z 2 topological order and the quantum spin Hall effect. *Physical review letters* 95.14 (2005), 146802.

[17] S.-Q. Shen. *Topological insulators*. Vol. 174. Springer.

[18] M. V. Berry. Quantal phase factors accompanying adiabatic changes. *Proceedings of the Royal Society of London. A. Mathematical and Physical Sciences* 392.1802 (1984), 45–57.

[19] X.-L. Qi, Y.-S. Wu and S.-C. Zhang. Topological quantization of the spin Hall effect in two-dimensional paramagnetic semiconductors. *Physical Review B* 74.8 (Aug. 2006). ISSN: 1550-235X. DOI: 10.1103/physrevb.74.085308. URL: http://dx.doi.org/10.1103/PhysRevB.74.085308.

[20] A. Burkov, M. Hook and L. Balents. Topological nodal semimetals. *Physical Review B* 84.23 (2011), 235126.

[21] A. Weststrom and T. Ojanen. Designer curved-space geometry for relativistic fermions in Weyl metamaterials. *Physical Review X* 7.4 (2017), 041026.

[22] M. Vazifeh and M. Franz. Electromagnetic response of Weyl semimetals. *Physical review letters* 111.2 (2013), 027201.

[23] L. Fu, C. L. Kane and E. J. Mele. Topological Insulators in Three Dimensions. *Phys. Rev. Lett.* 98 (10 Mar. 2007), 106803. DOI: 10.1103/PhysRevLett.98.106803. URL: https://link.aps.org/doi/10.1103/PhysRevLett.98.106803.

[24] B. A. Bernevig, T. L. Hughes and S.-C. Zhang. Quantum Spin Hall Effect and Topological Phase Transition in HgTe Quantum Wells. *Science* 314.5806 (2006), 1757–1761. ISSN: 0036-8075. DOI: 10.1126/science.1133734. eprint: https://science.sciencemag.org/content/314/5806/1757.full.pdf. URL: https://science.sciencemag.org/content/314/5806/1757.

[25] L. Fu and C. L. Kane. Topological insulators with inversion symmetry. *Physical Review B* 76.4 (2007), 045302.